Norwegian University of Life Sciences

Master's Thesis 2024 60 ECTS
Faculty of Chemistry, Biotechnology, Food Science (KBM)

Investigating the cardiac health of poultry suffering from wooden breast myopathy

Thea Kleiberg
Master's in biotechnology

Preface

The work of this master thesis was conducted at Nofima AS in Ås from August 2023 to May 2024 at the Department of Raw Materials and Process Optimization. The supervisors at Nofima were Sissel B. Rønning and Mona E. Pedersen, and Harald Carlsen was the supervisor from NMBU.

The interest in the project came as I first read the thesis description, as it is something never done before and as a project connecting molecular science with food science. I am very grateful for working on this project for a year; it has been fun and challenging.

I want to thank my Nofima Mona and Sissel supervisors for their good guidance every other week and their excellent spirit with the project. I also want to thank Harald for guiding the process. Moreover, I would like to thank Vibeke Høst, Tiril Aurora Lintvedt, Karen Wahlstrøm Sanden, and Jens Petter Wold at Nofima for their excellent help with the lab. Additionally, I would like to thank Cathrine Rein Carlson, Marianne Lunde and Thea Parsberg Støle for their great help at Ullevaal for the preparation and protein isolation of the samples.

My final thanks go to my family and friends for their support and advice and for keeping me in good spirits this year.

Ås, May 14, 2024

Thea Kleiberg

Table of contents

Abstract IV

Sammendrag VI

Abbreviations VIII

1. Introduction 1

1.1. Wooden Breast Myopathy 2

1.1.1. Duchenne muscular dystrophy 4

1.2. Heart Morphology 4

1.3. Muscle structure 5

1.3.1. Cardiomyocytes and myocardium 6

1.4. Extracellular matrix 7

1.5. Cytoskeleton 7

1.6. Mitochondria 8

1.7. Cardiac Failure 8

1.7.1. Cardiac Fibrosis 8

1.7.2. Cytochrome C in heart disease 11

2. Aim of the study 13

3. Material and methods 14

3.1. Background of the grouping of the heart samples used in this study 14

3.1.1. Preparation of tissue from heart samples for use in RNA and Protein extraction 14

3.2. Water holding capacity 16

3.3. Gene expression analysis using Q-PCR 16

3.3.1. Isolation of RNA 17

3.3.2. CDNA synthesis 18

3.3.3. Real-Time PCR 19

3.3.4. Calculating the relative mRNA expression 20

3.4. Protein expression analysis 20

3.4.1. Protein Isolation 21

3.4.2. SDS-gel electrophoresis 21

3.4.3. Sample preparation 21

3.4.4. Gel-electrophoresis 22

3.4.5. Blotting 22

3.4.6. Staining of membranes 23

3.4.7. Ponceau S 24

3.4.8. Quantification of western blot 25

3.4.9. SimplyBlue staining 25

3.5. Near Infrared (NIR) Spectroscopy to characterise fibrosis 26

3.6. Raman Spectroscopy for quality evaluation of tissue and collagen deposition 26
3.7. Differential gene expression analysis and Gene set enrichment analysis 27
3.8. Hubbard heart samples for a comparative analysis 28
3.9. Statistical analyses 29
4. Results 30
4.1. Wooden breast myopathy does not affect heart weight or property as water binding. 30
4.2. Spectroscopy 31
4.2.1. NIR spectroscopy 31
4.2.2. Raman spectroscopy 32
4.3. Gene expression analysis on fibrosis biomarkers 34
4.3.1. The relative gene expression of extracellular matrix proteins was unchanged 34
4.3.2. The gene expression of ECM enzymes and SDCs was similar in mild and severe WB samples 36
4.3.3. No significant increase or decrease in the gene expression of inflammation, cardiomyocyte, myofibroblast, cytoskeleton or the transforming growth factor (TGFB) in severe WB samples 38
4.4. Protein expression analysis 40
4.4.1. MMP2 but not troponin T protein expression was consistent with gene expression .. 40
4.5. RNA-Seq 41
4.5.1. Hierarchical clustered heatmap revealed groupings of gene expression 41
4.5.2. Gene Set Enrichment Analysis 42
4.6. The protein expression of Cytochrome C was significantly upregulated in severe WB samples 43
4.7. Comparative analysis Hubbard and Ross 44
4.7.1. Wooden breast's effect on Hubbard heart weight and water binding capacity 45
4.7.2. NIR spectroscopy 46
4.7.3. Collagen and fat deposition in Hubbard samples 47
4.7.4. SimplyBlue protein expression 50
4.7.5. MMP2 expression was higher in mild Ross samples 51
5. Discussion 53
5.1. Wooden breast-affected broiler chickens and the susceptibility to cardiac fibrosis 53
5.2. Hubbard and Ross hearts differ in protein pattern and fat compositions, which might be related to cardiac health 57
5.3. Methodical issues 58
6. Conclusion 59
7. Further research 59
8. References 60
9. Attachments 71

Abstract

The cause of wooden breast (WB) myopathy in broiler chickens is not well understood, but studies show it often develops into skeletal muscle fibrosis. In humans, muscle dystrophies, such as Duchenne muscular dystrophy (DMD), the patients often develop both skeletal muscle and cardiac fibrosis. If broiler chickens suffering from WB develop cardiomyopathies is still unknown. Therefore, the main aim of this study was to investigate if the cardiac muscle of wooden breast-affected Ross 308 broiler chickens shares the same molecular fingerprint for fibrosis as in the skeletal muscle.

Hearts of male Ross 308 broiler chickens of mild and severe WB were sampled. The heart samples were further cut, and the ventricular area was used to analyse cardiac fibrosis, as this area is often affected in cardiomyopathy. One part of the heart ventricle was used for RNA and protein isolation, and the other for spectroscopy analysis. Quantitative real-time PCR (qPCR), RNA-Sequencing (RNA-Seq) and western blotting were used to analyse gene and protein expression, whereas spectroscopic methods such as NIR and Raman were used to analyse the overall spectroscopic profile (physical fingerprint) of water, fat, and protein (collagen) deposition in the samples.

No signs of change in gene expression of fibrosis markers as extracellular matrix proteins, such as collagen, small leucine rich proteoglycans (SLRPs) or collagen crosslinking marker lysyl-oxidase (*LOX)* were observed at mRNA level in severe WB compared with mild WB. Raman analysis did not detect any change in spectral peaks of collagen, supporting the gene expression of collagen. The gene expression of tissue inhibitor of metalloproteinases 2 (*TIMP2*) was significantly downregulated in severe WB samples; however, this change was not observed at protein level by western blotting. Furthermore, no difference in gene expression of the syndecans, well known regulators of cardiac fibrosis, was observed between mild and severe WB affected chickens. No difference in gene expression of cardiomyocyte markers or cytoskeletal markers was obtained. Gene set ontology enrichment analysis (GSEA) of RNA-Seq data analysing the biological processes involved, detected mitochondrial, oxidative phosphorylation and ATP electron transport chain significantly downregulated in severe WB samples. Protein expression of cytochrome c (Cyt c) was then analysed by western blotting and was found to increase significantly in severe WB samples.

A smaller comparative analysis of chicken hearts was also performed between two chicken breeds: Hubbard JA787, a slow-growing breed, and Ross 308, a fast-growing breed, as growth

rate has been linked to WB myopathy in chickens. When we compared the hearts of mild WB affected animals of Ross 308 with the hearts of mild WB affected Hubbard JA787, we could clearly see differences in the chemical and physical composition by NIR and Raman, and different protein pattern by SDS-gel electrophoresis and Coomassie staining. MMP2 protein expression was higher in Ross 308, whereas Cyt c and Cardiac Troponin T (cTnT) were similar between mild WB groups of the two hybrids. Additionally, from visual observation, Hubbard JA787 hearts exhibited fat infiltration in their right and left ventricles. On the other hand, no fibrosis characteristics or mitochondrial dysfunction were found within Hubbard groups of mild and severe WB affected individuals based on NIR, Raman and western blot analysis.

In conclusion, the results did not indicate progression into fibrosis in the Ross 308 WB affected chicken hearts. However, signs of mitochondrial dysfunction were observed, which potentially can lead to the progression of heart failure. Fat infiltrations in Hubbard JA787 may indicate cardiac health problems.

Sammendrag

Årsak og molekylære mekanismer til wooden breast (WB) i kyllinger er fortsatt ikke godt forstått, men studier viser at det ofte utvikler seg til fibrose i skjelettmuskelen. Hos mennesker fører muskeldystrofier som Duchenne muskeldystrofi (DMD) ofte til kardiomyopati og muskel fibrose. Om WB affekterte kyllinger utvikler kardiomyopati er fortsatt uklart. Hovedmålet med denne studien var å undersøke om hjertemuskelen til WB affekterte Ross 308 kyllinger har samme molekylære fingeravtrykk for fibrose som skjelettmuskelen.

Prøver av hjerter til Ross 308 hannkyllinger med mild og alvorlig WB ble tatt ut. Hjerteprøvene ble så kuttet og ventrikkel området ble brukt til analyser av myokardfibrose, da fibrose ofte akkumulerer i dette området ved hjertesykdom. En del av hjerteventrikkelen ble brukt til RNA og proteinisolering, og den andre delen til spektroskopiske analyser. Kvantitativ real-time PCR (qPCR), RNA-Sekvensering (RNA-Seq) og western blotting ble brukt til å analysere genuttrykk og proteiner. NIR og Raman ble brukt til å analysere spektroskopisk profil (fysisk fingeravtrykk) av vann, fett og protein (kollagen) avsetning i prøvene.

Ingen tegn til endring i genekspresjon av fibrose markører som ekstracellulære matriksproteiner som kollagen, små-leucine rike proteoglykaner (SLRPs) og kollagen kryssbindingsenzym lysyl-oksidase (*LOX)* ble observert på mRNA nivå i alvorlig WB sammenlignet med mild WB. Raman-analysen detekterte ikke en endring i spektral topper av kollagen, som støtter genekspresjonen av kollagen. Genekspresjonen av vevsinhibitor av metalloproteinase 2 (*TIMP2*) var signifikant nedregulert i alvorlige WB-prøver, mens derimot på protein nivå ved western blot analyser ble denne endringen ikke observert. Videre, var ble ingen forskjeller i genekspresjon av syndekaner som er kjente regulatorer av myokardfibrose, observert mellom mild og alvorlig WB affekterte kyllinger. Ingen forskjeller i genekspresjon av kardiomyocytt markører eller cytoskjelett markører ble funnet. Gensett ontologi berikelsesanalyse (GSEA) av biologiske prosesser påviste at mitokondrielt genuttrykk, oksidative fosforyleringen og ATP-elektrontransportkjeden var betydelig nedregulert i alvorlige WB-prøver. Protein uttrykket av cytokrom c (Cyt c) ble så analysert ved western og ble funnet signifikant økt i alvorlige WB prøver.

En mindre komparativ analyse av kyllinger ble utført mellom to kyllingeraser i tillegg: Hubbard JA787, en saktevoksende rase og Ross 308, en rasktvoksende rase, da rask vekst har blitt koblet til WB myopati i kylling. Når vi sammenlignet hjertene av milde WB affekterte

kyllinger av Ross 308 med hjertene av milde WB affekterte til Hubbard JA787, kunne vi se klare forskjeller kjemisk og fysisk sammensetning fra NIR og Raman, og annerledes protein mønster fra SDS-gel elektroforese og Coomassie farging. MMP2 protein ekspresjonen var høyere i Ross 308, mens Cyt c og kardialt Troponin T (cTnT) var like mellom mild WB gruppene av de to hybridene. I tillegg, fra visuell observasjon, Hubbard JA787 hjertene viste fett infiltrasjon i deres høyre og venstre ventrikkel. På en annen, side ble ingen fibrose karakteristikker eller mitokondriell dysfunksjon funnet i Hubbard gruppene av mild og alvorlig WB individer basert på NIR, Raman og western blot analyser.

I konklusjon, resultatene indikerte ikke progresjon til fibrose i Ross 308 WB affekterte kylling hjerter. Derimot, tegn til mitokondriell dysfunksjon ble observert, som mulig kan lede til progresjon av hjerte feil. Fett infiltrasjon i Hubbard JA787 kan indikere hjerteproblemer.

Abbreviations

ARVC	Arrhythmogenic right ventricular myocardium
BGN	Biglycan
COL1A1	Collagen type I
COL1A3	Collagen type 3
cTnT	Cardiac Troponin T
Cyt c	Cytochrome c
DCN	Decorin
DES	Desmin
DMD	Duchenne muscular dystrophy
ECM	Extracellular matrix
GSEA	Gene set enrichment analysis
IL1B	Interleukin- 1 beta
LOX	Lysyl-Oxidase
LUM	Lumican
MMPs	Matrix metalloproteinases
NIR	Near Infrared
PDGFRb	Platelet-derived growth factor receptor beta
qPCR	Quantitative Polymerase reaction
RNA-Seq	RNA-Sequencing
SD	Standard deviation
SDS	Sodium dodecyl sulphate
SLRPs	Small leucine-rich proteoglycans

TIMPs	Tissue inhibitors of metalloproteinases
TLR4	Toll-like receptor 4
TNNT2	Troponin T 2
TPM2	Tropomyosin 2
TUBA1A	Tubulin alpha 1-chain
TUBB1	Tubulin beta 1-chain
WB	Wooden breast

1. Introduction

The consumption of chicken meat has increased tremendously worldwide in the last 40-50 years due to its low cost and high nutritional value. Consuming chicken meat also agrees with most religions and cultures' ethics, increasing sales value. Subsequently, the demand for poultry meat has increased, which has triggered a breeding selection for effective poultry meat production for broiler Ross 308 (Petracci et al., 2019).

The broilers of Ross 308 reach slaughter weight faster, have higher breast yield, and need less feed than other breeds. However, the genetic factors driving the fast growth rate have introduced some adverse health concerns (Forseth et al., 2023). Muscle alterations such as wooden breast syndrome (WB) are prevalent in Ross 308, and the pathological hallmarks of WB include skeletal muscle fibrosis and lipidosis together with myofiber degradation and inflammation (T. Xing et al., 2021). These changes in morphology in broiler chickens impact food quality parameters with hardening and stiffness of the breast muscles and pale colour (Petracci et al., 2019).

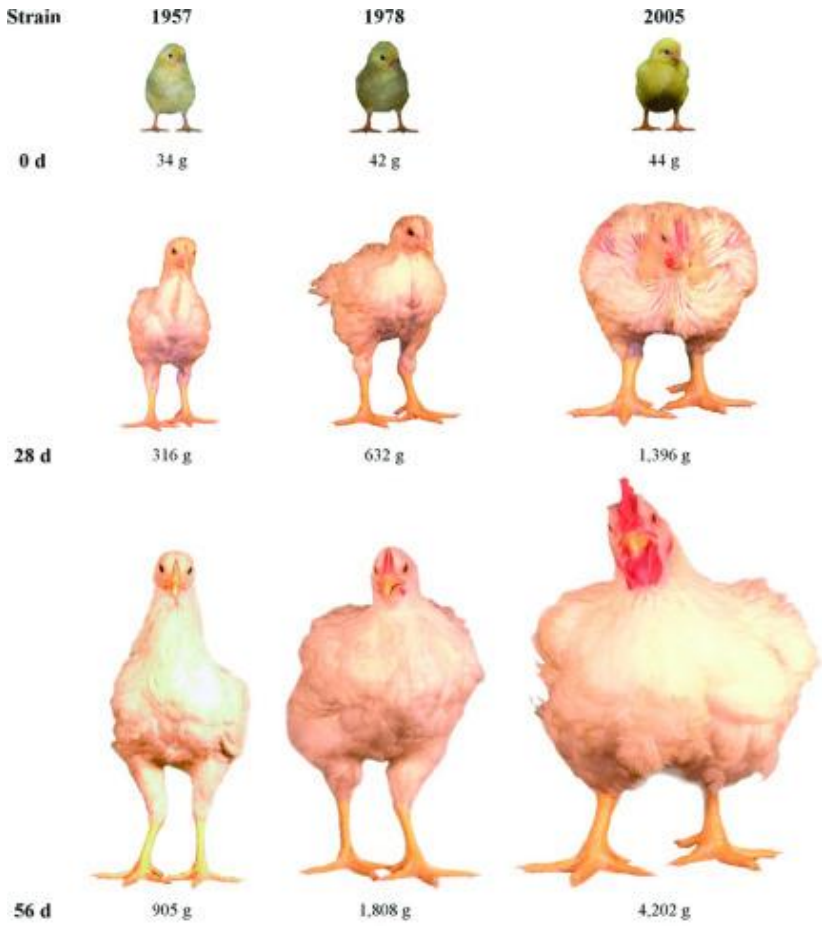

Figure 1.1. Ross 308 broiler chickens age-related growth from 1957 to 2005. *Figure retrieved from (Zuidhof et al., 2014).*

Research conducted under experimental conditions has linked broiler's fast growth to high mortality (Dixon, 2020; Havenstein et al., 2003). Moreover, studies show that broiler chickens had compromised adaptive immune systems, more metabolic disorders, skeletal issues, and exhaustion. Additionally, the broilers exhibited decreased activity levels, more foot pad lesions and hock burns, and deteriorated feather conditions observed in broiler chickens (Forseth et al., 2023).

Petracci et al.,2015 suggested that the fast growth rate found in broiler chickens', specifically in the breast muscle, advances to unmanageable pressure on the metabolism of the muscle, which then prompts degenerative features like Duchenne muscular dystrophy (DMD). Patients with DMD develop weakness in both the skeletal and cardiac muscles and exhibit morphological characteristics such as myofiber degradation and fibrosis, as in wooden breast myopathy. Cardiomyopathy has become a leading death cause of DMD (Lechner et al., 2023). Furthermore, myocardial fibrosis occurs before global dysfunction in the left ventricle in DMD patients (Walcher et al., 2011). However, the extent of WB on the broiler's cardiac health remains unclear, and if WB myopathy shares some similar characteristics as DMD affecting both the skeletal muscle and heart function.

1.1. Wooden Breast Myopathy

In the last ten years, wooden breast (WB) myopathy has become more prevalent in broilers. Broiler chickens' effective breeding for fast growth and high breast yield has resulted in chicken breeds that may achieve body weight up to 2.0 kg in just 32 days, with a fifth of the birds' total weight being the breast meat. Furthermore, from 1957 to 2005, the feed conversion ratio was reduced by 50% (Zuidhof et al., 2014). Consequences of myopathies such as WB are poor meat quality, impaired appearance, and texture. The characteristic traits of WB include a pallid appearance, pronounced toughness, and often a surface that displays a translucent fluid (Sihvo et al., 2014). Additionally, the breast fillets affected by WB also, when processed, can cause issues with low water holding capacity (Geronimo et al., 2019; Mazzoni et al., 2015; Soglia et al., 2016).

Moreover, WB fillets exhibit chemical alterations in protein and mineral content, consequently leading to an increase in the lipids and water content (Geronimo et al., 2019; Mazzoni et al., 2015; Sihvo et al., 2014; Soglia et al., 2016). Since consumers do not accept WB fillets' quality as meat products, WB fillets are used for ground products or animal feed (Petracci et al., 2019; Xing et al., 2020). Recently, consumers have become more aware of

myopathies in fast-growing broilers, and the welfare of animals in meat production has become of higher concern (Petracci et al., 2019).

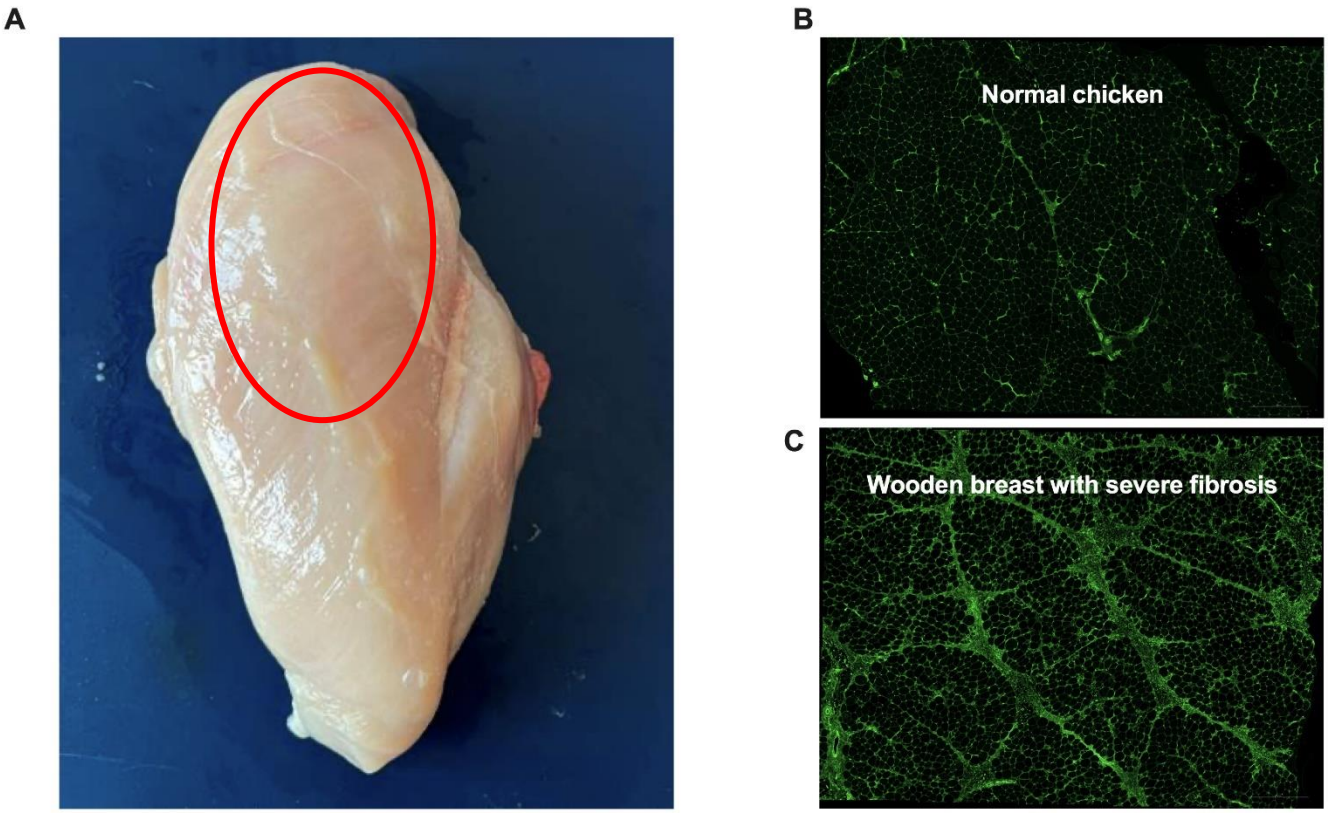

Figure 1.2. Chicken breast fillet and histology showing wooden breast myopathy. *(A) An image of a chicken breast fillet affected by wooden breast myopathy; the red circled area shows the WB affected area. (B) Microscopy image of normal chicken breast fillet (left). (C) wooden breast affected breast fillet with severe skeletal muscle fibrosis(right). Labelled using WGA (green, stains the connective tissue). Sample from a commercial line in Norway. Photo©Nofima.*

Even though WB has introduced considerable problems to the poultry industry, its aetiology is poorly understood. Genetic selection has been suggested to cause WB due to the chickens' fast growth rate and high breast yield. Severe skeletal muscle fibrosis, necrosis and multifocal degeneration of the muscle tissue are morphological characteristics of WB, which have been demonstrated by several studies (Soglia et al., 2016; Velleman & Clark, 2015). Evidence shows muscle fibre cross-sections of different sizes compared to non-affected, including hypertrophic cells. Diminished angiogenesis and adipose infiltrations have also been demonstrated (Soglia et al., 2016; Velleman & Clark, 2015). Alterations such as these are associated with processes of inflammation and muscle fibre degeneration (Mazzoni et al., 2015; Sihvo et al., 2014; Soglia et al., 2016).

Fibrosis is a common pathological feature of WB-affected broiler chickens' and a characteristic hallmark. The process behind fibrosis results from chronic tissue injury and

inflammation, with the additional excessive extracellular matrix deposition (ECM) deposition (T. Xing et al., 2021). ECM components such as collagens, fibronectin 1, and small leucine-rich proteoglycans (SLRPs) and tissue regulators as syndecans are increased in skeletal muscle fibrosis in WB affected broilers (Pejšková et al., 2023). Collagen accumulation is often responsible for the hardness of the affected broiler tissue (Sihvo et al., 2014).

1.1.1. Duchenne muscular dystrophy

Skeletal muscle fibrosis, like that observed in WB-affected broilers, shows similarities with DMD in humans (Petracci et al., 2015). DMD is a severe muscular dystrophy found in 1 in 3500 male births; a mutation in dystrophin makes the patients unable to walk around age 10-12. Later in life, the patient develops respiratory and cardiac muscle diseases.

Cardiomyopathy is becoming the leading death cause in DMD patients. The patients exhibit skeletal muscle and cardiac muscle myopathies. Cardiomyopathy develops as the patients reach adulthood, often resulting in myonecrosis, fatty substitution, fibrosis, or chronic inflammation. It is still unknown how cardiomyopathy influences the disease course in DMD (Lechner et al., 2023). Characteristics of cardiomyopathy in DMD are normal or thinned left ventricular wall thickness, with an ongoing decrease in ejection fraction or fractional shortening (Judge et al., 2011). The morphology seen in the skeletal muscle DMD can be reminiscent of WB.

1.2. Heart Morphology

The heart is a muscular pump that works by moving blood to the peripheral organs and back again to transport nutrients and clear waste products from the tissues of the body. The heart comprises four chambers: two thin-walled atrium and two thick-walled ventricles. The atrium is located right above the left and right atrium. The ventricles execute most of the work in the heart. Subsequently, the atria gather blood from the lungs, and the venous system contracts it and then expels it to the ventricles. Afterwards, the ventricles pump blood through the body and into the lungs (Shah et al., 2009).

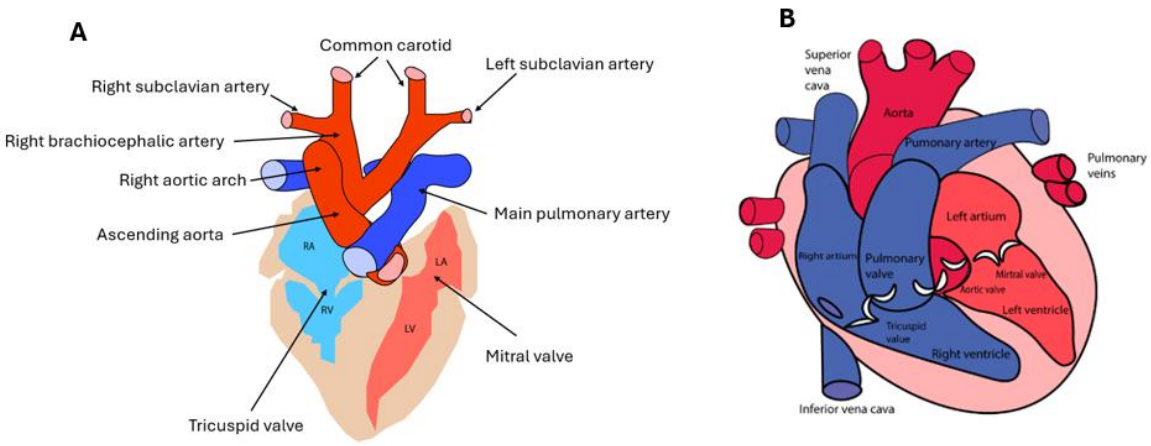

Figure 1.3. The structure of the chicken and human heart has some differences. *The human heart has an internal cavity separated into four chambers: the right and left atrium and the right and left ventricle. The atrium is thinned wall, and the ventricles are thick-walled. The thickness of the heart chambers is due to the amount of myocardium. The right ventricle in chickens is significantly smaller than the left ventricle**.** However, the human heart has the same structure with four chambers and valves**.** Modified after (Wittig & Münsterberg, 2020) in Adobe Illustrator.*

Both humans and chickens have four chambers in the heart, which consist of the right and left atrium and the right and left ventricles, as shown in Figure 1.3. Additionally, both species have four valves, and their circulation is similar. However, there are some structural and physiological differences. In chickens, the heart rate and body temperature are higher. Also, both chicken ventricles have a higher muscle mass relative to the chamber size, and the left ventricular is substantially larger than the right ventricular. This allows for five times the systemic pressure found in humans (Wittig & Münsterberg, 2020).

1.3. Muscle structure

The heart's primary duty is pumping blood throughout the circulatory system. The cardiac muscle consists of myofibrils, which convert chemical energy into mechanical energy. This conversion allows the heart to perform work and generate force. These myofibrils are oriented parallel to the cell axis and consist of transverse stripes called sarcomeres. Sarcomeres are composed of two distinct components: the contractile proteins and the cytoskeletal proteins. The thin actin and thick myosin filament proteins control myofilaments contraction and produce the force necessary to pump blood. The presence of Ca^{2+} and ATP facilitates the cooperation regulation. Moreover, the thin filament regulatory troponin-tropomyosin complex

binds to actin, controlling the cooperation to ensure the smooth operation of the cardiac muscle (Sequeira et al., 2014).

Cardiac muscle shares similarities with skeletal muscle, such as the presence of muscle fibres with striated appearances and the use of thick and thin contractile filaments. These give each cell type its distinctive striated appearance. The cardiac muscle is mononucleated and contains cross striations made by the alternate segments of the thick and thin protein filaments anchored by Z-lines. Conversely, the cardiac muscle is shorter than the skeletal muscle. Both actin and myosin are primary structural proteins, as illustrated in Figure 1.5 (Shah et al., 2009).

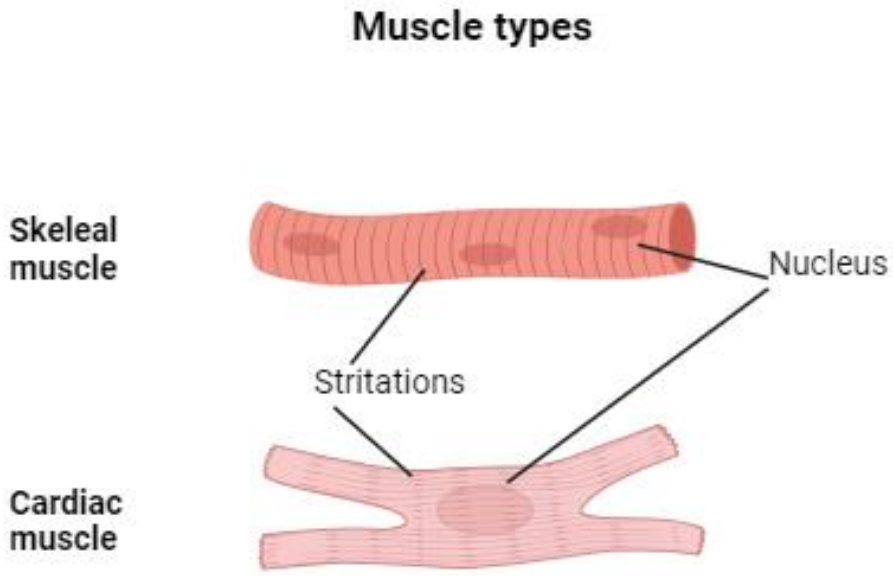

Figure 1.5. Skeletal and cardiac muscles share similarities, but there are some differences. *The skeletal muscle and cardiac muscle have muscle fibres with striated appearances. The cardiac muscle is shorter than the skeletal muscle and has small regenerative potential after birth. Created in Biorender.com.*

However, there are some essential differences between skeletal and cardiac muscle. The skeletal and cardiac muscles have distinctive differences in terms of their physiological and regenerative potential. The mammalian heart has minimal repair capacity after birth. In contrast, the skeletal muscle has a regenerative potential through quiescent muscle satellite cells activated upon injury (Xie et al., 2017).

1.3.1. Cardiomyocytes and myocardium

Cardiomyocytes are known as the most energetic cells in the body, and they are responsible for constantly contracting without exhaustion (Severs, 2000). The cardiomyocytes consist of

separate subcellular areas: the intercalated disc, the lateral sarcolemma, the cytoskeleton, and lastly, the cellular organelles. The cardiomyocyte has a cylindrical shape, which often branches and connects to neighbouring cardiomyocytes along the longitudinal axis, intersecting the intercalated discs. Moreover, the cardiomyocytes have a striated appearance with one or two centrally located slightly elongated nuclei (Sarantitis et al., 2012).

Several cell types are present within the cardiac muscle, including fibroblasts, the most abundant cells in the normal heart, and endothelial and smooth muscle cells. Surrounding the cardiomyocytes are different layers of extracellular matrix: the inner layer is the endomysium, then the perimysium, and the outermost layer is the epimysium (Sarantitis et al., 2012).

1.4. Extracellular matrix

The skeletal and cardiac muscles have an adequate ECM network and share similar structure and function (Purslow, 2008). The ECM is crucial for the structure and function of a healthy heart. In addition, the ECM also has a role in cardiomyocyte differentiation, division and growth (Macfelda et al., 2007). Moreover, the ECM consists of different molecules such as collagens, fibronectin, fibrillin, proteoglycans and hyaluronan (Lockhart et al., 2011). Particularly, the ECM structures and function of the endomysium and perimysium are comparable in skeletal and cardiac muscle (Purslow, 2008).

1.5. Cytoskeleton

The cytoskeleton in cardiomyocytes provides structure and mechanical help and spatial assembly of other subcellular components (Sarantitis et al., 2012). Additionally, the cytoskeleton intervenes in signalling. Hence, the cytoskeleton can alter gene expression and protein synthesis (Frank et al., 2006; Kostin et al., 2000).

Proteins in the cytoskeleton participate in the cell's structural integrity, shape, and mechanical resistance. Four groups of proteins are found in the cytoskeleton, divided based on their function and structure. The first group are the sarcomeric skeleton proteins, which include titin, C-protein, α-actinin, myomesin, and M protein. The second group is true cytoskeletal proteins such as desmin, actin and tubulin. The third group is membrane-associated proteins like ankyrin, vinculin, spectrin, talin and dystrophin. The fourth and last group is the protein of the intercalated disc, which includes desmosomes, desmin and also proteins associated with the adherent junction with N-cadherin, vinculin, catenin and connexin (Hein et al., 2000).

1.6. Mitochondria

The mitochondria are the cell's powerhouse and, therefore, are essential for energy production in cardiomyocytes. In cardiomyocytes, mitochondria are found between myofibrils and below the sarcolemma (Gustafsson & Gottlieb, 2007). Mitochondria supply ATP (A. Li et al., 2020), critical to supporting the contraction and relaxation sequences. They also carry out other significant tasks, such as cell death signals, calcium buffering, and synthesis of cellular components (Torrealba et al., 2017).

Mitochondria's major role in cardiac cells is to produce ATP through oxidative phosphorylation (Gustafsson & Gottlieb, 2007). Moreover, mitochondria regulate oxidative stress, promote cell survival, and modulate apoptotic death (Siasos et al., 2018).

1.7. Cardiac Failure

Conditions where the heart cannot supply blood to organs and tissues are characterised as heart failure (Sequeira et al., 2014). Cardiac failure can be of pathophysiological or function perspectives. Affected areas include the circulatory system and the cardiac function or underlying pathophysiological factors (Tanai & Frantz, 2016). The final common pathway of cardiovascular diseases is heart failure, which includes sustained pressure overload, myocardial ischemia or infraction, volume overload, and, lastly, inherited and acquired cardiomyopathies (Hilfiker-Kleiner et al., 2006). To compensate for a failing heart, the heart has different mechanisms to maintain sufficient function (Kemp & Conte, 2012). The heart remodels itself short-termly as a coping mechanism for increased demands. On the other hand, long-term remodelling leads to abnormalities and heart failure (Ponikowski et al., 2014)

A dysfunctional heart is a consequence of cardiac remodelling. Subsequently, changes in the cellular and molecular levels change, leading to ventricular dysfunction and heart failure. Some pathophysiological factors involved in the remodelling of the heart are cell death, energy metabolism, oxidative stress, inflammation, collagen, contractile proteins, calcium transport and neurohormonal activation (Azevedo et al., 2016).

1.7.1. Cardiac Fibrosis

Fibrosis is a condition characterised by the accumulation of ECM in the cardiac muscle and is a pathological remodelling of the ECM (Frangogiannis, 2021; Hinderer & Schenke-Layland, 2019). The accumulation of ECM proteins causes systolic and diastolic dysfunction (Kong et al., 2014). The heart has limited regenerative capacity, and the ventricles often undergo ECM-remodelling in fibrosis and further form scarring in response to the sudden death of

cardiomyocytes. The reparative myofibroblast, the main producer of ECM, is triggered by inflammation and leads to the formation of a collagen-based scar. However, fibrosis can occur in the interstitial space in some cardiac diseases without substantial cardiomyocyte loss. Additionally, ageing, obesity, and diabetes promote fibrosis in the myocardium and can reduce ventricular fulfilment (Frangogiannis, 2021).

Fibrosis in the heart causes changes in the amount of ECM proteins, which impacts the heart's function. Collagen type I and III accumulation is a hallmark of cardiac fibrosis. Both collagen types are increased in a fibrotic heart, regardless of what caused the fibrosis. The expression pattern of the two collagen types depends on various factors (Kong et al., 2014). Besides, an increase in collagen type I has been suggested to increase the stiffness of the myocardium. Reduced ventricle compliance has been associated with increased deposition of collagen I fibres (Frangogiannis, 2021).

Lysyl-oxidase is a protein found in the extracellular matrix and has the role of cross-linking collagen fibrils (López et al., 2010). Lysyl-oxidase is a family of enzymes responsible for extracellular collagen cross-linking in cardiac fibrosis (Frangogiannis, 2021). Upregulation of lysyl-oxidase has been observed in myocardial stiffness, dysfunctional left ventricular and heart failure (López et al., 2010).

In nearly all forms of heart failure, cardiac fibrosis is a requisite component characterised by the accumulation of ECM proteins in the myocardium. Additionally, cardiac fibrosis alters the myocardial architecture, the myocardial excitation-contraction coupling, and the systolic and diastolic function. Moreover, the seriousness of cardiac fibrosis and high long-term mortality are related in patients with heart failure (Li et al., 2018). Under pathological conditions, the ECM proteins are exposed to changes, which alters the architecture of the matrix. Subsequently, the activation, migration, and proliferation of cardiac fibroblast to myofibroblast (SMA expressing) are transformed. Cardiac myofibroblasts play a significant role in the development of cardiac diseases preceding to heart failure (Li et al., 2018). Fibroblast and myofibroblast activate the secretion of collagens, following the procollagen chains that are processed and made into fibrils and then cross-linked (Frangogiannis, 2021).

In a healthy heart, the cardiac ECM consists of fibrillar collagen I and III, the primary structural proteins composing the framework. Other components in normal adults' hearts are proteases and inhibitors such as metalloproteinases (MMPs), tissue inhibitors of metalloproteinases (TIMPs), and small leucine-rich proteoglycans (SLRPs) such as biglycan,

lumican, and decorin regulators of collagen fibrillogenesis (Christensen et al., 2019). Also, nonstructural glycoproteins and glycosaminoglycans are found in the cardiac ECM. Alterations to ECM components are involved in the pathogenesis of cardiac fibrosis and ventricular dysfunction (Li et al., 2018).

One of the most significant enzymes in degrading the ECM components is the MMPs, and MMP-2, -9, and -13 are the subtypes found in the heart. MMPs proteolytic activity is regulated by TIMP, moreover, TIMP 2,3 and 4 are all found in normal adult hearts(Li et al., 2018). TIMPs role is inhibiting activated MMPs to keep the homeostatic balance in the myocardial ECM. Additionally, TIMP2,3 and 4 have been observed to enhance myocardial fibrosis, while TIMP1 has an inverse impact on fibrosis (Takawale et al., 2017).

A regular occurrence in cardiac remodelling is subsequent remodelling of the ECM. The remodelling of the ECM causes dysfunction in the interaction involving the myocardia cells and the blood vessels, compromising the structural integrity and function of the cardiac muscle. Moreover, the overproduction and accumulation of ECM proteins follow an increased myocardium stiffness and impair the contraction and relaxation of the ventricles (Fan et al., 2012). The remodelling of the ECM components of the cardiac muscle alters the ventricular wall and chamber dimensions (Brower et al., 2006)

Fibrillar collagen is a stiff material that, in contact with other myocardial components, has a significant role in the maintenance of the size, shape, and function of the ventricles. Degradation of collagen often results in dilation of the ventricles and decreased ventricular stiffness. On the other hand, an increase in interstitial collagen concentration or cross-linking results in a stiffer myocardium and diastolic dysfunction of the ventricles (Brower et al., 2006). The degradation of collagen is a crucial step in remodelling the ECM, which MMPs control. MMPs are a family able to digest a variety of ECM enzymatically and are present in the heart (D'Armiento, 2002).

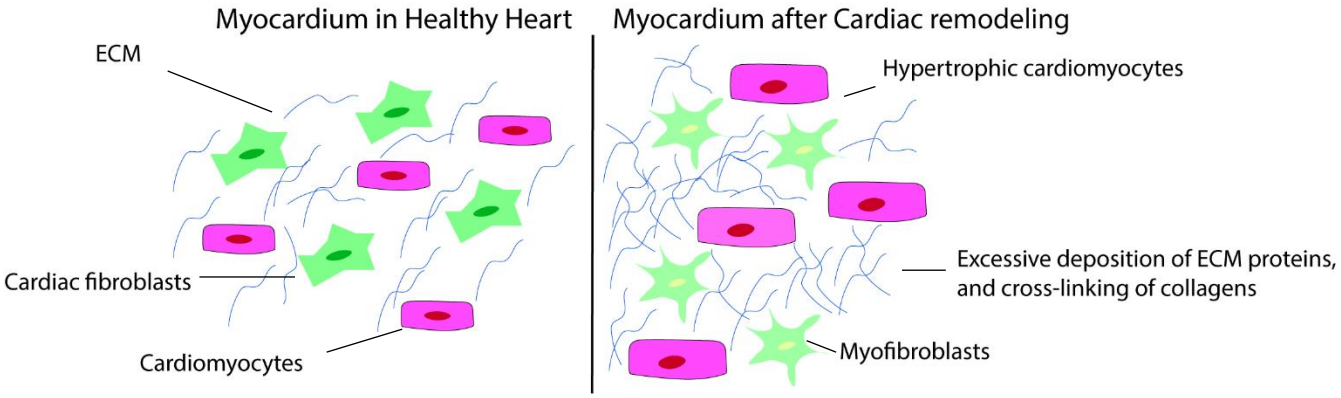

Figure 1.6. The myocardium in a healthy heart consists of cardiomyocytes, cardiac fibroblasts, and the extracellular matrix. Under pressure overload, the myocardium remodels, which introduces the accumulation of the ECM proteins with collagen cross-linking. Moreover, enlarged cardiomyocytes and differentiation of fibroblasts into myofibroblasts are also events leading to fibrosis. Modified after (Andenæs, 2022) in Adobe Illustrator.

Fibrosis and ECM remodelling due to pressure overload puts mechanical stress on the ventricles and thus may initiate hypertrophy and fibrosis. The mechanical stress is transferred to the ECM, and then cell ECM ties may lead to the remodelling of the ECM. Further, the remodelling can activate the intracellular signalling pathways, which results in cardiac hypertrophy, fibrosis, and apoptosis (Fan et al., 2012).

SLRPs have been indicated to have a significant role in the adult heart, and reduced levels demonstrated a loosely structured ECM. Increased levels of lumican have been found in fibrotic tissues. Lumican has a role in binding and organisation of collagens. Moreover, biglycan and decorin normally found in a healthy adult heart and have been found increased in tentative models of heart failure. Regulating fibrillogenesis, and binding collagens are roles of biglycan and decorin (Christensen et al., 2019).

Syndecans are transmembrane proteoglycans that transmit signals during fibrogenic processes mediated by growth factors. Moreover, syndecan has four isoforms that were all suggested to be increased during myocardial infarction in mice. Syndecan-1 expression is also suggested to increase during tissue injuries and regulates the inflammatory and reparative responses. More importantly, the absence of syndecan-1 causes disorganisation of collagen and destruction. Subsequently, this lead to increased MMP2 and MMP9 activity (Lunde et al., 2016).

1.7.2. Cytochrome C in heart disease

Dysfunction of the mitochondria has been linked to different cardiac diseases, such as hypertrophy, hypertension, ischemia/reperfusion, and heart failure (Torrealba et al., 2017). Abnormal mitochondrial dynamics are associated with failing cardiomyocytes, increasing

oxidation stress, and impairing Ca^{2+} handling. Both are essential in myocardial remodelling, leading to heart failure (Verdejo et al., 2012).

Cytochrome c resides in the mitochondria in healthy cells, where its primary function is as an electron carrier in the electron transport chain. It is a highly conserved globular protein found in animals, plants, humans, and bacteria. Mitochondrial cytochrome c has four essential functions: electron transport, peroxidase activity, redox regulation, and regulation of the mitochondrial physiological functions (Zhou et al., 2024).

The globular protein has distinct functions when it translocates to the cytoplasm, nucleus, or ECM. Additionally, irregular cytochrome c signalling participates in several pathological conditions and diseases. Cytochrome c release and mutations are associated with various human diseases, and the expression of cytochrome c may work as a biomarker in diseases. When released into the extracellular space, the protein can be used as an in vivo marker for mitochondrial damage after heart failure (Zhou et al., 2024).

2. Aim of the study

Poultry production uses genetic selection of faster-growing chickens to meet the increased demand for poultry meat, which has introduced severe health concerns in broiler chickens such as Ross 308. One of the introduced health concerns that not only worsens the meat quality but also the health of the broiler chickens is wooden breast, a myopathy that often develops into skeletal muscle fibrosis. Wooden breast is characterised by white striping, transparent thick fluid, and white bulges, and are evidently hard**.** In human muscular dystrophies, such as Duchenne muscular dystrophy, the patients often develop both skeletal muscle and cardiac fibrosis. Whether chickens suffering from WB also develop cardiac failure is still unclear. Therefore, the main goal of this study is to investigate if the cardiac muscle of Ross 308 chickens shares the same molecular fingerprint for fibrosis as the skeletal muscle. Since growth rate has been associated with WB, we also wanted to compare the hearts of Ross 308 with the more slow-growing chicken breed Hubbard since these are less prone to develop WB.

The main hypothesis for this thesis has been:

- Wooden breast-affected broiler chickens are more susceptible to cardiac fibrosis than non-affected chickens.
- The slow-growing Hubbard JA787 has a healthier heart than the fast-growing Ross 308.

Subgoals of the thesis are to:

- Investigate functional properties (water-binding properties, collagen deposits and protein content) by spectroscopic methods.
- Assess cardiac fibrosis by investigating the same fibrotic markers found in skeletal muscle, i.e., ECM proteins, MMPs, TIMPs, syndecans, and cytoskeleton markers, through qPCR and western blotting
- Perform bioinformatic analysis on an RNA-Seq dataset comparing WB and healthy chicken.
- Compare the fast-growing breed Ross 308 with the slower-growing breed Hubbard

3. Material and methods

3.1. Background of the grouping of the heart samples used in this study

The heart samples analysed in this study were from an ongoing project (Chicken-Health NFR 323939) to characterise the molecular background of wooden-breast pathogenesis and fibrosis in breast fillets (*Petroralis major*) in male Ross 308. A chicken trial triggering wooden breast using male Ross 308 fed a *libitum* diet from 10 days of age was performed as described in Pejšková et al., 2023., and slaughtered at 36 days post-hatching. The breast fillets were characterised and classified according to the degree of WB and fibrosis standardised by methods by usage as NIR (Wold et al., 2019) and from histology by haematoxylin and eosin (HE)-staining described in Pejšková et al., 2023. Moreover, 12 chickens were diagnosed with WB, 13 without WB in this chicken trial, and the heart samples used in this study followed the same classification.

3.1.1. Preparation of tissue from heart samples for use in RNA and Protein extraction

Heart samples collected in the chicken trial (Figure 3.1) were weighed immediately after slaughtering and further dissection. The ventricular area of the heart is often affected with fibrosis in cardiomyopathy, and therefore this area (Figure 3.1) was kept and stored at -80℃ for all further analysis in this thesis. Frozen ventricle samples were in addition also dissected into smaller samples for the different analyses, as described in Figure 3.2. However, all smaller samples contained at least one part of the base, mid, and apex to gain homogenous samples.

Figure 3.1. The heart samples before dissection. *The heart samples were dissected as marked by the black line, before put in storage at -80℃.*

Method:

- To obtain a homogeneous sample, the heart samples were carefully sectioned to include tissue from the heart's base, mid, and apex. Sectioning was done using Electrolux medical refrigerator MRF120/35 at -30℃ to keep the material frozen to prevent degradation of the samples before further RNA and protein isolation.
- The samples were split into parts A and B, as shown in Figure 3.2.
- Part A was used to extract RNA and protein from the heart tissue and contained equal amounts of left and right ventricles.
- Part B had a smaller amount of the right ventricle and was placed in a zip bag. Part B was stored in zip-lock bags at -80℃ until further analysis with NIR and Raman spectroscopy.

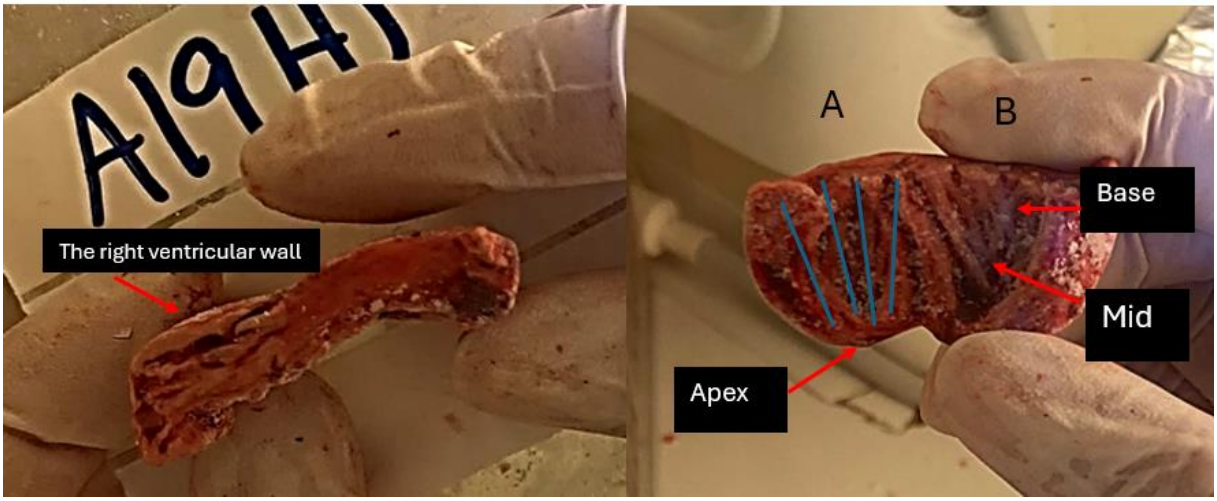

Figure 3.2. Section area (cross direction and longitudinal) of heart used in RNA and protein extraction. The left and right ventricles. *Part A was used to extract RNA and protein from the heart tissue and contained the base, mid, and apex with equal amounts of left and right ventricles. Part B contained the right ventricle and was placed in a zip bag before NIR and Raman spectroscopy analysis. The ventricle with most of the right ventricle was cut downward to get the base, mid, and apex of the ventricle. This secured the most homogenous solution possible. Part A was split into four parts and put into cryo tubes for storage at -80℃ before RNA and protein extraction.*

- Furthermore, part A was cut vertically with a scalpel/knife into four parts (Figure 3.2). The four parts were divided into four to six pieces and then placed into cryogenic tubes. An equal amount of tissue from base, mid and apex was allocated for RNA and protein analysis. Thus, both RNA and protein lysation were made more accessible.

3.2. Water holding capacity

Broilers with WB are known for alterations in moisture content and water-holding capacity in their breast fillets (Choi et al., 2024). The procedure described below was carried out to investigate the water properties of the heart of WB-affected chickens. The water holding capacity was determined by weighing heart samples frozen after storage at -80℃ and after thawing at 4℃ overnight in a refrigerator.

Method:

- The falcon tubes were weighed before heart samples were allocated to the tubes. The falcon tube weight was subtracted from all measurements.
- The (B) part of the heart samples were weighed, frozen, and thawed in falcon tubes.
- Water from the thawed heart samples was also weighed in falcon tubes.
- The water holding capacity was calculated from equation 1, shown below:

$$(1)\ WHC(\%) = \frac{Defrosted\ heart\ (g)}{Frozen\ heart\ (g)} \times 100$$

3.3. Gene expression analysis using Q-PCR

The relative mRNA expression was quantified using real-time polymerase reaction (Q-PCR). Quantitative RT-PCR measures the amplified DNA target during the PCR, not its end, as in conventional PCR. The reactions are monitored during the exponential amplification phase, and users can determine the number of copies of the template DNA. A fluorescent reporter molecule (probe) is added in each reaction, yielding increased fluorescence with an increasing amount of DNA. This enabled us to monitor the fluorescence signal as amplification occurs; the fluorescent dyes yield an increasing signal proportional to the number of PCR product molecules generated. Each amplification cycle doubles the number of target molecules that theoretically amplifies the DNA exponentially. RT-PCR measures the amount of DNA from the fluorescent dyes after each cycle. Each cycle has three general steps: denaturation, annealing, and extension. During denaturation, high-temperature incubation melts the double-stranded DNA into single strands. Eventually, the secondary structure is looser in single-stranded DNA. In the next step, annealing, the complementary sequences can hybridize, and the proper melting temperature is calculated based on the primers used. The temperature in the last step extension is at 70-72℃; the DNA polymerase activity here is optimal. Primer extensions have a rate of around 100 bases per second (Scientific, 2014).

3.3.1. Isolation of RNA

Materials:

- RNAeasy® Fibrous Tissue Mini kit (50)

Method:

- The frozen heart samples were thawed on ice and then placed in tubes containing 300µL Buffer RLT and porcelain beads to disrupt and homogenize the tissue. The tubes were placed in a Precellys® 24 tissue homogenizer for two times 20 seconds.
- Then 590µL nuclease-free water and 10µL proteinase K were added and mixed before the tubes were incubated at 55°C for 10 minutes. The tubes were then centrifuged at 10.000 rpm for 3 minutes.
- The supernatant was then transferred to a new tube, and 0.5 volumes of 96-100% ethanol were added and mixed. 700µL of the sample was then transferred to an RNAeasy Mini column placed in a 2mL collection tube. The tubes were then centrifuged for 15 seconds at 17.000 rpm. The flow-through was discarded, and the step was repeated until complete lysation.
- 350µL Buffer RW1 was added to the RNAeasy column and was centrifuged for 15 seconds at 17.000 rpm, and the flow-through was discarded.
- 10µL DNAse was mixed with a stock solution of 70µL Buffer RDD added to an RNAeasy membrane and incubated for 15 minutes at 20-30°C.
- Then 350µL Buffer RW1 was added to the RNAeasy column. Flow-through was discarded.
- 500µL Buffer RPE was subsequently added to the RNAeasy column, centrifuged again for 15 seconds at 17.000 rpm, and discarded the flow-through.
- Then 500µL Buffer RPE was added to the RNAeasy column and centrifuged for 2 minutes at 17.000 rpm.
- The RNAeasy column was placed in a new 1.5mL tube. 50mL of RNAse-free water was added, and the tube was subsequently centrifuged for 1 minute at 17.000 rpm.
- Yield was measured on Nanodrop, and RNAse-free water was used as a blank. 2µL of the isolated RNA sample was used for measuring.
- The isolated RNA samples were allocated to new Eppendorf tubes for storage at -80°C.

3.3.2. CDNA synthesis

In molecular biology, cDNA synthesis is an important method, and it can be valuable in single- and double-stranded forms. Additionally, cDNA is equivalent to genomic DNA and is a product of synthesis using RNA as a template. The enzyme DNA polymerase, also known as reverse transcriptase (RT), makes the first strand of cDNA. RNA tends to degrade quickly; single- or double-stranded DNA can be kept in the freezer indefinitely. Furthermore, by cloning cDNA, it is possible to generate as much cDNA as desired. Both long and short cDNA molecules can be used to find specific genes or sequences in DNA libraries (Farrell, 2010).

Method:

- Firstly, the cDNA was diluted according to the Nanodrop values. The RNA sample was diluted to 0.5µg/µL per sample. The dilutions were done on a 96-well PCR plate. The appropriate amount of the respective sample was added to the well, followed by the right amount of nuclease-free water. The total volume of water and RNA sample was 10µL.
- The cDNA synthesis was prepared as described below in Table 1.

Table 1. Supermix used for cDNA synthesis for each sample.

Reagent	**Volume(µL)**
LunaScript® RT Supermix	4
RNA sample	2
Nuclease-free Water	14
Total volume	20

- 2µL of each diluted RNA sample was pipetted into a new 96-well PCR plate. Then, 4µL of LunaScript RT Supermix was pipetted into each well, as well as 14µL nuclease-free water, and was mixed well by pipetting up and down. The total volume of the sample was 20µL.

- The 96-well PCR plate was sealed and then put in GeneAmp®PCR System 9700 with three cycle steps. The first cycle was primer annealed at 25℃ for 2 minutes. Then, the cDNA synthesis at 55℃ for 10 minutes. Lastly, the heat inactivation at 95℃ for 1 minute.
- The cDNA was diluted again before real-time PCR to ensure the right amount for all the probes. The samples were diluted with 130µL of nuclease-free water. The total volume of the samples was 150µL, and the concentration of cDNA was 7.5µg/µL.
- The samples were placed at -20℃ until real-time PCR.

3.3.3. Real-Time PCR

Method:

- The qPCR was prepared as described in the Table 2 below.

Table 2. Protocol for typical qPCR analysis. For each experiment the cDNA is prepared fresh.

Reagent	**Volume(µL)**
Luna Universal Probe qPCR Mix	5
TaqMan probe	0.5
Template cDNA	2
Nuclease-free Water	2.5
Total volume (µL)	10

- TaqMan Probes and the Luna Universal Probe qPCR Master mix were thawed at room temperature and, subsequently put on ice. Both components were inverted or gently vortexed.
- New Eppendorf tubes were marked with the corresponding probe.
- 400µL Luna Universal Probe qPCR mix was pipetted into each Eppendorf tube, then mixed with 200µL nuclease-free water.
- 40µL of each TaqMan probe was added to an Eppendorf tube and mixed gently by pipetting.
- The Eppendorf tubes were then kept on ice before plating on 384-well qPCR plate.

- The prepared cDNA was thawed on ice and then 30µL of the first 12 cDNA samples was aliquoted from a 96-well PCR plate to a 384-well qPCR plate by using a ClipTip Equalizer pipette, leaving 15 wells with 2µL of cDNA each. The same procedure was repeated twice to get all the 24 samples transferred to the 384-qPCR well plate.
- 8µL of the corresponding master mix was pipetted with Multipipette onto the 384-well plate in three replicates.
- The qPCR plate was then sealed with a transparent film.
- The plate was then spanned at 1000 rpm using a Megafuge 8 centrifuge for 1 minute to remove bubbles and collect the liquid.
- After centrifugation, the qPCR plate was then put in QuantStudio5.
- Real-time qPCR was set up with three cycle steps. The first is the initial denaturation at 95℃ for 60 seconds for 1 cycle. Then, the denaturation at 95℃ for 15 seconds, the extension cycle at 60℃ for 30 seconds for 40-45 cycles. The recommended cycle profile "Fast" was used. After one hour, the results were exported.

3.3.4. Calculating the relative mRNA expression

The relative mRNA expression was calculated using a method retrieved from Schmittgen & Livak. The Ct values were first exported to Excel. Then, the average of the Ct values from the technical triplicates was subtracted from the Ct value of the reference gene. The relative gene expression was then calculated using $2^{-(\Delta Ct \text{ gene of interest} - \Delta Ct \text{ reference gene})}$ (Schmittgen & Livak, 2008).

3.4. Protein expression analysis

An essential method to detect protein is western blotting (Kurien & Scofield, 2015) Western blotting is a technique which is antigen specific for monoclonal antibodies (Burnette, 2009). First, sample proteins are separated by size on a denaturing gel. Then, the proteins are transferred to a membrane, also recognised as a procedure called western blotting. Furthermore, the proteins will form the same pattern as the gel on the membrane (Kurien & Scofield, 2015). Then, the membrane is put in a blocking agent, which is important to remove any unspecific bindings on the membrane (Kothari & Mathews, 2015). Subsequently, the membrane is coated with primary antibodies. If the primary antibody binds to the protein on the membrane, it can be visualised by adding a secondary antibody. The process behind the binding and visualisation of primary and secondary antibodies depends on two things, which are the specificity and the ability of the antibody to recognise and bind to the target protein.

Signals on western blots can detected by fluorescence, where the secondary antibody is labelled with fluorophore (Pillai-Kastoori et al., 2020). This way the signals can be visualised by an instrument.

3.4.1. Protein Isolation

The protein was isolated at the Institute of Experimental Medical Research (IEMR) at Oslo University Hospital Ullevaal. The method used for protein isolation is described in (Støle et al., 2022):

Method:

- The tissue from the left ventricle of the chicken hearts was homogenised with TissueLyser with 20mM Hepes ice-cold lysis budder, 150mM NaCl, 1mM EDTA, and 0.5% Triton-X100.
- A Complete EDTA-free protease inhibitor cocktail and PhosSTOP were added to the mix.
- Furthermore, the homogenate was centrifuged at 14.000 rpm for 10 minutes at 4℃.
- After centrifugation, the supernatant was stored at -80℃.
- The supernatant protein concentrations were then determined using the Micro BCA protein assay kit.

3.4.2. SDS-gel electrophoresis

High-resolution sodium dodecyl-sulfate polyacrylamide gel electrophoresis (SDS-PAGE) is often used to separate complex mixtures of proteins. The SDS-PAGE method denatures the proteins using anionic detergent, which binds to the proteins and separates them due to their negative charge relative to their molecular mass. Furthermore, the electrophoresis separates the proteins based on molecular mass via a porous acrylamide gel matrix (Nowakowski et al., 2014).

3.4.3. Sample preparation

Method:

- The samples were thawed at room temperature.
- Then the samples were centrifuged for 20 minutes at 13 000 rpm to collect supernatant.
- The supernatant of each sample was then transferred to new Eppendorf tubes and then mixed with 40µL DTT and 50µL NuPAGE® LDS Sample Buffer (4X) and distilled water.

- The samples were then put on a heating block at 70℃ for 10 minutes before loading on gel.

3.4.4. Gel-electrophoresis

Method:

- NuPAGE™ 10% Bis-Tris Gel was placed in the Invitrogen NuPAGE Novex® Mini cell System.
- Running buffer was made using 25mL MOPS diluted in 500mL Milli-Q water. The middle chamber was filled first with a running buffer to ensure no leakage in the system; the outer chamber was then filled.
- 2µL of ECL Plex Rainbow ladder was used as a marker and pipetted into the first well in the gel. Then 20µL of each sample was pipetted one by one into the wells. The gel system was then used with 200V for about 45 minutes.
- Meanwhile, the blocking solution was prepared with 100mL TBS-T and 2g Amersham ECL Blocking agent. The solution was then placed to stir for 30 minutes. TBS-T was also prepared using 1 tablet of TBS-T and 500mL Milli-Q water.
- The gel system was stopped when the protein bands had wandered down the entire gel. The gel cassette was opened with a cassette opener, and the thick part of the gel was cut.

3.4.5. Blotting

The blotting was done using the iBlot™3 Western Blot transfer device and the iBlot 3 Western Blot Transfer System (Invitrogen™).

Method:

- The gel was transferred to a nitrocellulose membrane on the Anode stack, and moist filter paper was put on top. Then, to prevent air bubbles, the paper was rolled with a blotting roller.
- The cathode stack was then placed on top of the stack and rolled again with a blotting roller to prevent air bubbles. Then, a disposable sponge was placed on top.
- The anode stack was then placed in the iBlot™3 device, which was closed, and the blotting procedure was ready to start.
- The blotting program for a broad range for 6 minutes was used, and then after the stack was dissembled, only the nitrocellulose membrane was kept.

3.4.6. Staining of membranes

Method:

Table 3. Primary antibodies were used for protein expression analysis.

Primary antibodies	**Dilution**	**Species**	**Molecular size(kDa)**
MMP2	1:1000	Rabbit	66-72
Cardiac Troponin T	1:500	Mouse	40
Cytochrome C	1:2000	Mouse	17

Table 4. Secondary antibodies were used in the protein expression analysis.

Secondary antibodies	**Dilution**	**Target species**
ECL™Plex goat-a-mouse IgG, Cy™3	1:2500	Mouse
ECL™Plex goat-a-rabbit IgG, Cy™5	1:2500	Rabbit

- For each blot, 3mL 0.2% ECL Advance™ blocking agent diluted in TBS-T was pipetted into a 50mL falcon tube before adding primary antibodies.
- Membrane was washed 2x5 minutes with TBS-T on tilt.
- The primary antibodies were made in a 0.2% ECL Advance™ blocking agent diluted in TBS-T, and then the appropriate dilution volume of the primary antibody of interest was added.
- The blot was then incubated in primary antibodies by being added to the falcon tube with tweezers and then put on a rolling mixer for 1.5 hours at room temperature or overnight at 4℃.

- The blot was then rinsed twice in TBS-T and washed 2x5 minutes with TBS-T on a rolling mixer.
- Secondary antibodies were then made with the correct antibody dilution to 3mL of 0.2% ECL Advance™ blocking agent diluted in TBS-T. The falcon tube was then put on a rolling mixer for 1 hour. Here, it is essential to shed the light.
- The blot was then rinsed three times with TBS-T and washed 2x10 minutes with TBS-T while on a rolling mixer.
- Then, the blot was dried on filter paper in the dark.
- The dried blot could be scanned in a Syngene G:Box Chemi XX6 with the appropriate fluorescent light.

3.4.7. Ponceau S

Normalisation is needed to quantify the relative target protein of a western blot. Earlier housekeeping genes have been utilised as a reference to normalise western blots. Normalisation of the blot is necessary to lower mistakes such as uneven loading errors and inadequate sample preparation. Commonly used housekeeping proteins used for normalisation are glyceraldehyde 3-phosphate dehydrogenase (GAPDH), β-actin, or α-tubulin, which are all expressed at high levels and can be used with different target antibodies both at the same probing as the target protein or after stripping the blot. During quantification the abundance of the housekeeping protein is used to normalise the amount of target protein in each sample. Ponceau S can be used for total protein normalisation and poses advantages over housekeeping protein normalisation. Moreover, Ponceau S is not dependent on antibodies and is reversible. Moreover, Ponceau S uses signals from several proteins in one sample lane in contrast to one when using housekeeping protein (Sander et al., 2019).

Method:

- The nitrocellulose membrane was put in a small gel tray, then filled with Ponceau S staining ready-to-use solution until the membrane was fully covered.
- The solution was incubated for 5-10 minutes before being washed with distilled water until the background of the blot was white to attain the best visibility of the total protein.
- The blot was then scanned using visual light in Syngene G: Box Chemi XX6.
- Bands of different molecular weights of the protein of interest were quantified and then used to attain a normalised value.

3.4.8. Quantification of western blot

The bands were quantified using ImageQuant™800, an image software used for gel and blots to determine the protein concentration. Ponceau S staining was used to normalise the value of the proteins of interest in each sample. Equation 2 was used to calculate the relative protein concentration:

$$(2)\ N = \frac{S}{R}$$

N is the normalised value, R is the amount of reference protein from the Ponceau S, and S is the band intensity of the protein of interest from the desired blot.

Method:

- The relative protein concentration was determined using a scanned blot image. The image was then inverted so that the signal of the bands was coloured blue.
- The lanes were then defined and drawn. To reduce any background signal, Rolling ball-2 was utilised.
- The bands were then detected manually. The results were then exported to Excel before normalised against Ponceau's quantification of the same blots.

3.4.9. SimplyBlue staining

SimplyBlue™ SafeStain can be used to visualise protein expression in polyacrylamide gels. The method is highly sensitive and provides results quickly (Invitrogen, 2001).

Method:

- NuPAGE 4-12% Bis-Tris gel was used for SimplyBlue staining of the protein samples to allow good protein separation.
- The gel was loaded with 10µL of 40µg samples together with 10µL Benchmark Prestained standard.
- The gel was rinsed three times for 5 minutes with 100mL distilled water to remove SDS and buffer salts that can interfere with the dye. Each rinse was discarded.
- 30mL SimplyBlue solution was added to cover the mini gel. The gel was incubated for 2 hours, and bands began to develop. The stain was discarded afterwards.
- The gel was then washed with distilled water overnight to obtain the most precise visualisation for photography.
- The stained gel was then scanned in Epson perfection.

3.5. Near Infrared (NIR) Spectroscopy to characterise fibrosis

Near Infrared (NIR) spectroscopy is a rapid, non-intrusive optical method used to detect fibrosis via changes in the tissue composition. NIR spectroscopy measures the absorption of the electromagnetic radiation of wavelength from 750 nm to 2500 nm. It detects absorption of the overtones and combinations of vibrational modes associated with C-H, O-H, AND N-H chemical bonds. The molecular bonds absorb electromagnetic radiation, and NIR measures the absorption within 750 to 2500 nm. Furthermore, it generated a spectrum that was distinct for each sample. The spectrum indicates organic molecules' chemical and physical characteristics within the sample and provides valuable insights into the composition (Prieto et al., 2017).

Karen Wahlstrøm Sanden and Jens Petter Wold conducted the NIR analysis and helped interpret the result.

Method:

- Samples were weighed and then thawed overnight at 4℃ before being weighed once more and measured with an NIR instrument.
- The NIR instrument was blanked before use.
- The heart samples were placed on a black background to prevent any background signal.
- The instrument was blanked occasionally between measurements.
- All samples were measured twice at the ventricular area from both mild and severe WB groups.

3.6. Raman Spectroscopy for quality evaluation of tissue and collagen deposition

Raman spectroscopy can provide more detailed information about chemical and molecular interactions. It allows for non-destructive analysis and is more versatile than other spectroscopy methods. The signal from Raman spectroscopy is more reliable and of better quality than infrared spectroscopy, especially when the sample contains water. In situ, quality control of fish, meat, and liquids is one of Raman spectroscopy's usages in the food industry (Orlando et al., 2021).

Raman spectroscopy is more specific than NIR spectroscopy, and structural changes in collagen conformation can be detected. Alterations in the collagen molecule cause several diseases, such as fibrosis. Changes in collagen are the hallmark of fibrosis and are one of the

main components of the ECM in connective tissues. Since collagen type I exhibit a fibrillar structure attributed to the triple-helix arrangement of the polypeptide chains, the minuscule fibres come together to create fibrils. Raman spectroscopy demonstrates sensitivity to two secondary structures found in collagen macromolecules, the α-helix and the β-sheet structure. The secondary structures provide the structure and the stability of the collagen fibrils. The frequency of Amide I and III bands can detect alterations in the secondary structures. The 1672 and 1650 cm-1 Amide I bands can reflect these changes (Martinez et al., 2019).

Tiril Aurora Lintvedt helped perform the Raman analysis and interpret the result.

Method:

- The samples were weighed, frozen, and thawed, then kept at room temperature before measuring.
- Samples were then placed on an aluminium plate and measured for 25 seconds with the Raman laser twice with constant motion at the ventricular area to obtain two replicates of each sample of mild and severe WB.

3.7. Differential gene expression analysis and Gene set enrichment analysis

A differential expression can be used to find genes expressed differently between conditions using RNA-Seq data. Different methods exist to perform a different expression analysis of RNA-Seq data (Soneson & Delorenzi, 2013). This study used a parametric method, DESeq2, in R Studio.

Method:

- The RNA-Seq read counts were first exported from Excel into R Studio.
- Firstly, the genes were tested for overdispersion by the negative binomial model, and genes with a total count under 10 were removed.
- The count data was then rounded to integers
- DESeq2 was then run on the count data, and DESeq2 estimated the size factors, dispersions, and gene-wise dispersion. DESEq2 also replaced outliers and refitted for 294 genes.
- The counts from the DESeq2 analysis were then normalised, and the result could be summarised and ordered by the p-adjusted value.

- The Z score of all the top 20 genes was calculated before the genes were plotted in a hierarchal clustered heatmap.

Following the differential gene expression analysis, a gene set ontology analysis (GSEA) could be done. Performing a level of statistics is the first step in a GSEA, and this is to identify gene sets that are increased and decreased from the RNA-Seq (Hung et al., 2011).

Method:

- First, the Fast Gene Set Enrichment Analysis (fgsea), the genome-wide annotation for chicken (Gallus gallus) from Bioconductor (org.Gg.eg.db), clusterProfiler, and AnnotationDbi package was loaded into R Studio.
- Furthermore, the differential expression analysis result was sorted in descending order based on the values of the stat column.
- Moreover, a vector called gene list with the values from the stat column was created.
- Then, the GSEA was performed using the gene list vector, with enrichment scores provided from the fgsea method and a p-adjusted value for multiple testing using the Benjamini-Hochberg method for false discovery rate correction.

3.8. Hubbard heart samples for a comparative analysis

Norsk Kylling AS distributed Hubbard JA787 heart samples to our study to perform a comparative analysis between two chicken breeds. Hubbard JA787 is a slower-growing breed than Ross 308. Several experimental studies have shown that Hubbard has fewer health issues than Ross 308, although wooden breasts are also detected in this breed. Due to transportation problems, the heart was left at room temperature and not on dry ice for a couple of days, and therefore, RNA was not isolated from the Hubbard samples. 10 mild WB samples and two severe WB samples were used in this study, as Norsk Kylling AS only obtained two severe WB affected chickens on the day of the slaughter.

- The Hubbard hearts were incised differently from the Ross heart samples. Subsequently, the protein lysate contained more of the right ventricle than in Ross. However, since the left ventricle is more prominent than the right ventricle, the lysate will contain most of the left ventricle.
- The heart samples were separated into two sections, as in Ross, where part A was used for protein isolation and histology, and part B was used for NIR and Raman spectroscopy.

- Part A was cut into four parts, as in the Ross samples. The parts were then sectioned into four to six pieces before being placed in cryogenic tubes.
- Half of the tissue pieces were allocated for protein isolation, a quarter of the heart tissue was placed in zip bags for histology, and the last quarter was kept as remains.
- Part B was placed in zip lock bags for storage at -80℃ before NIR and Raman analysis.

3.9. Statistical analyses

The results of all analyses were presented in bar charts, and the average and standard deviation were calculated and presented in error bars. Moreover, a two-tailed unpaired Welch's t-test was performed to prove significance in Excel and GraphPad Prism, with $p<0.5$ considered statistically significant.

4. Results

4.1. Wooden breast myopathy does not affect heart weight or property as water binding.

Cardiac diseases such as hypertrophy and fibrosis can increase heart mass (Zhu et al., 2022). Therefore, the weight of whole heart collected after slaughter of the two groups, mild and severe was compared. As seen from Figure 4.1A, no significant difference in the weight of the hearts was obtained.

WB myopathy is well-known to influence the water-binding properties in breast fillets, as revealed by NIR-spectroscopy (Wold et al., 2019). For investigating water binding, each sample was weighed as frozen (Figure 4.2B) and defrosted overnight at 4°C (Figure 4.2B). Furthermore, the water binding capacity for the frozen weight was subtracted from the defrosted weight to determine the water binding capacity (Figure 4.2D). No significant difference was observed between the groups, although the tendency showed that the severe WB group had slightly higher weight compared with the mild WB group.

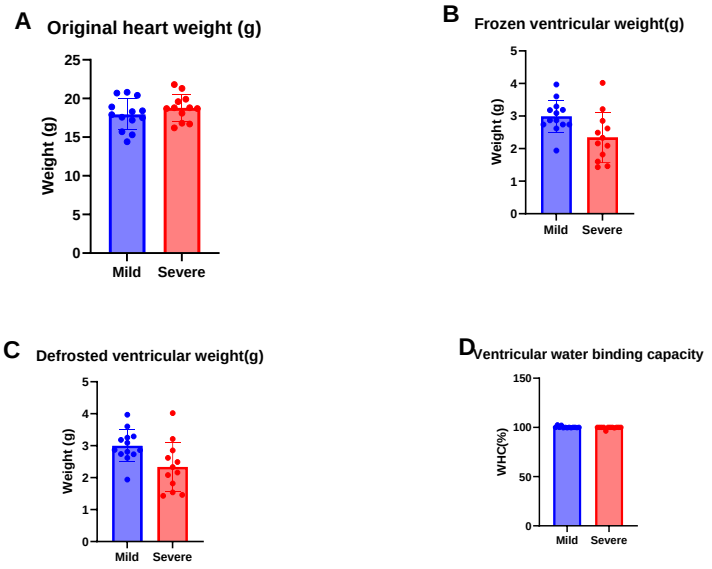

Figure 4.1 Measurement of heart weight and water binding capacity in normal and WB individuals. *(A) The heart samples original weight (g) immediately after slaughter. (B) Frozen weight of the ventricles. (C) The weight of the ventricles defrosted with water. (D) Water binding capacity (%) of the ventricles. The bar shows the average for each group (n=25), the dots illustrate each sample, and the error bars are the SD. Welch's t-test observed no significant difference between the two groups.*

As shown in Figure 4.1D, the severe WB group did not have reduced water binding capacity compared to the mild group.

4.2. Spectroscopy

The heart ventricles were analysed using two spectroscopy methods to investigate potential molecular fingerprints related to water-binding, protein, collagen, and fat.

4.2.1. NIR spectroscopy

NIR spectroscopy determined the heart samples' water-binding, protein, and fat deposition.

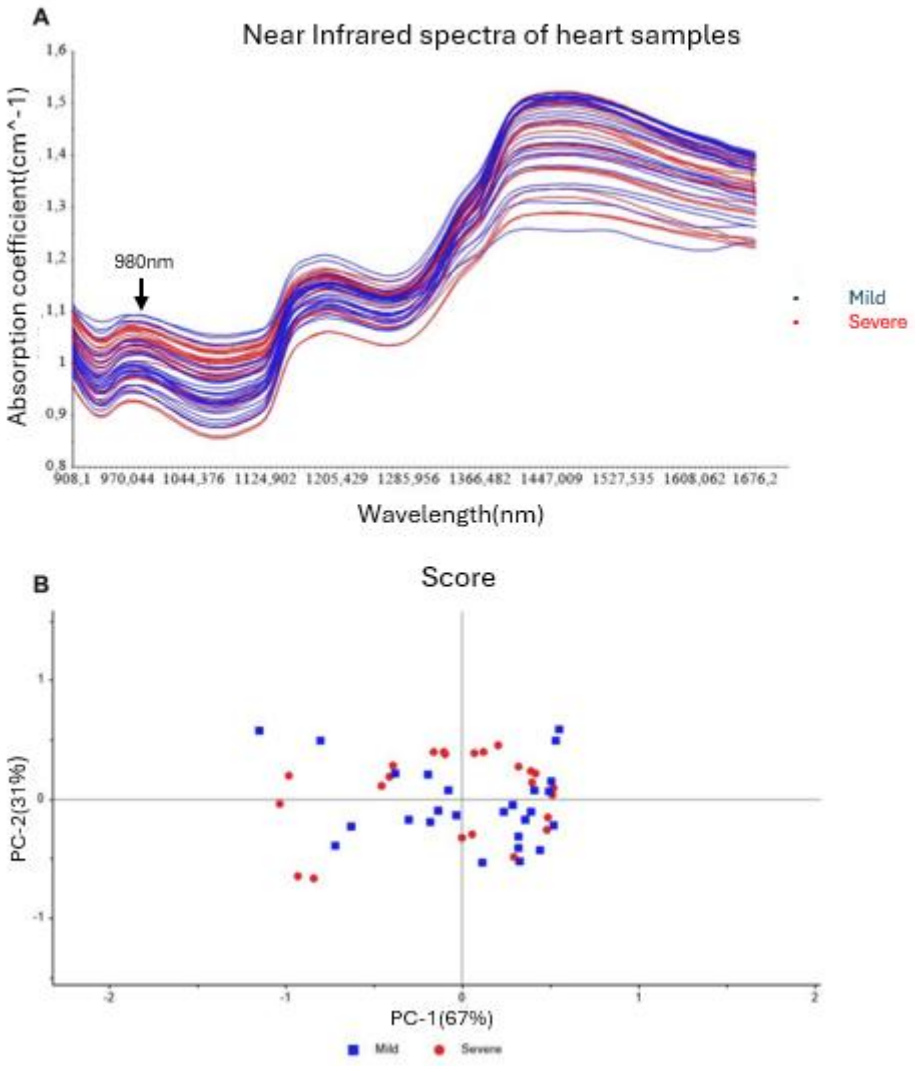

Figure 4.2 No significant differences in water, proteins, and fat were found in the groups (A), and PCA Component Analysis demonstrated similarities across groups (B). *(A) Raw data absorption spectrum of the Ross heart samples affected by wooden breast dystrophy. The x-axis demonstrates the light absorption of each sample (cm^{-1}), while the y-axis shows the wavelength (nm). The peak at 980 nm shows moisture content in the samples, which indicated no difference in water content between the two groups. (B) Principal Component Analysis (PCA) was performed on the NIR data to provide insight into the patterns and variations present in the dataset. Severe and mild WB samples displayed similarities, and there was no clear sorting between the two groups.*

The samples used for analysis of water-binding in section 4.1 were further analysed by NIR. An observation was conducted: both the mild and severe WB samples demonstrated similar consistent trends in their water-binding with no constituted shift in the absorption peak at approximately 980 nm, presented in Figure 4.2A.

From the PCA analysis, the groups showed similarities in the spectral peaks of water, protein, and fat. The mild and severe WB samples grouped (Figure 4.2B) which indicated similar chemical or physical structures.

4.2.2. Raman spectroscopy

Raman spectroscopy allowed the investigation of collagen accumulation in the severe WB group due to fibrosis in the heart tissue.

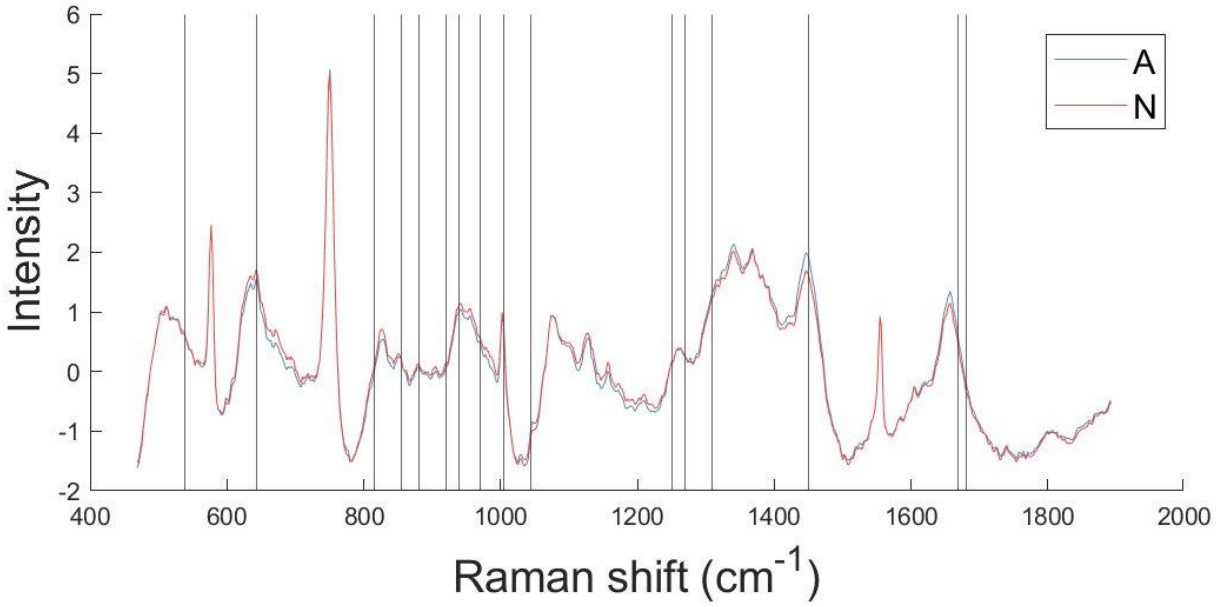

Figure 4.3. Collagen peak intensity ratios showed no significant difference in collagen accumulation between the groups. *Average Raman intensity spectrum of Ross samples. The ratios 827/854, 919/936, 1657/1678, and 1315/1340; are peaks where collagen can be measured. No significant difference in collagen deposition was found between the groups. The spectra are baseline corrected, and SNV normalised.*

Results obtained from the Raman spectroscopy indicate an absence of evident collagen accumulation or upregulation across both mild and severe WB samples. Under examination, no collagen peak intensity ratios indicated heightened collagen in the mild versus severe WB samples presented in Figure 4.3.

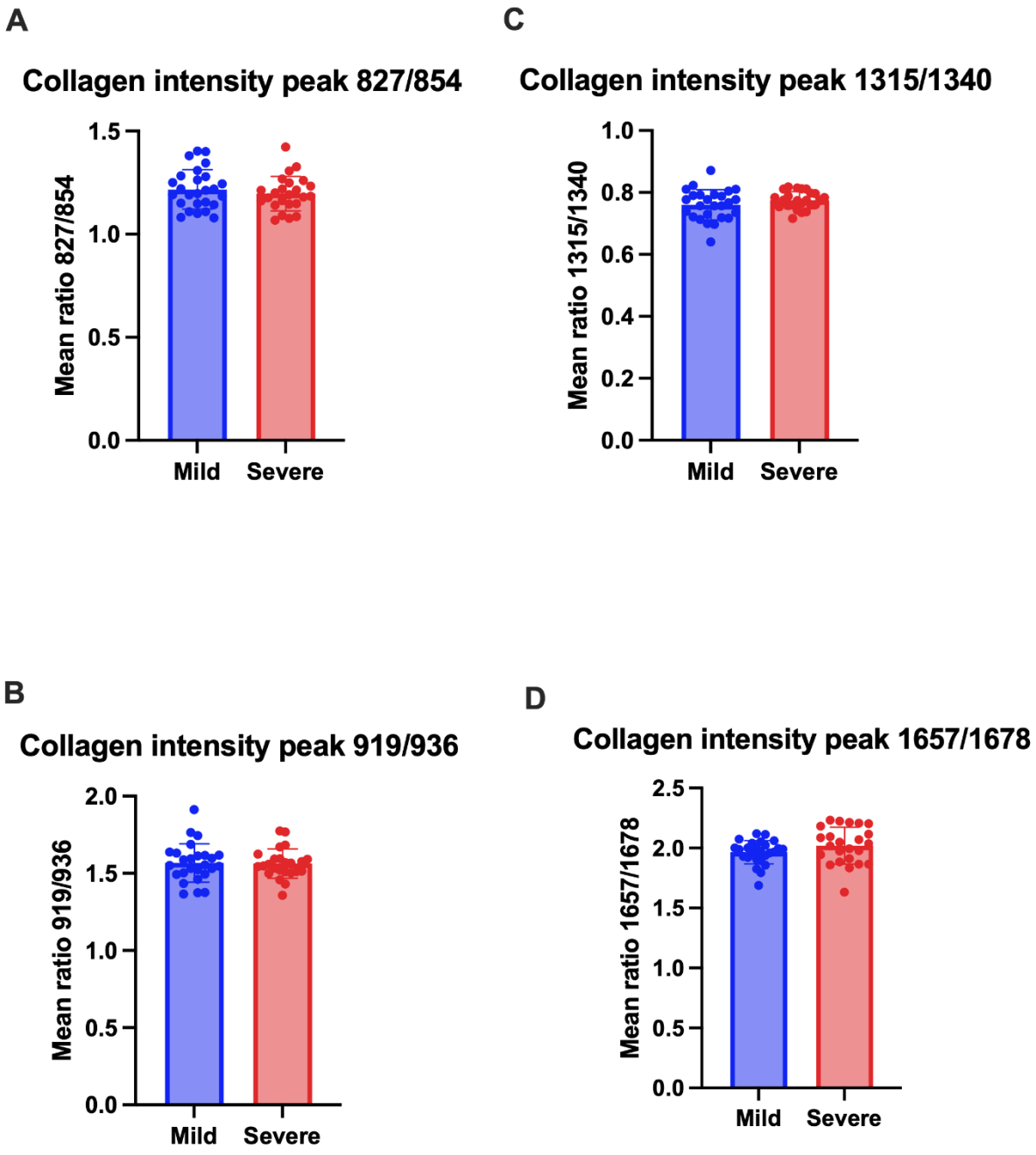

Figure 4.4. No collagen accumulation was observed in the groups. *The collagen peaks of Raman spectroscopy were done on the ventricles of the mild and severe WB groups. Samples were measured twice at the ventricular area with the Raman laser instrument with a constant moving motion. The intensity ratios (A) 827/854, (B) 919/936, (C)1315/1340, and (D) 1657/1678 show alterations in the collagen macromolecule. The average of each sample signal was calculated, and an unpaired Welch's t-test found no significant difference between mild and severe groups. The error bars illustrate the SD. The dots represent each sample signal.*

The collagen deposition in the ventricles of mild and severe WB samples seemed to be at normal levels, as shown in Figure 4.4 A-D. There was no trend of collagen accumulation in the severe WB samples as an effect of fibrosis. The level of collagen seemed similar in both conditions.

4.3. Gene expression analysis on fibrosis biomarkers

WB is often characterised by fibrosis, the accumulation of ECM proteins (Frangogiannis, 2021). The gene expression of ECM matrix proteins was analysed to investigate the presence of fibrosis.

4.3.1. The relative gene expression of extracellular matrix proteins was unchanged

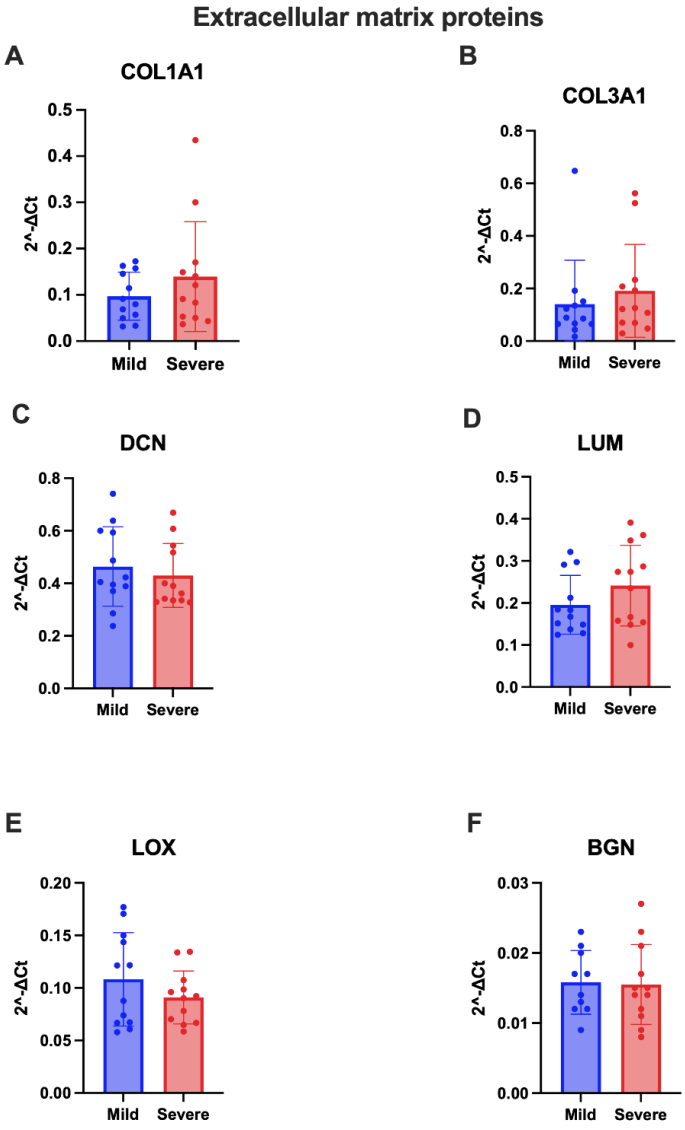

Figure 4.5. Gene expression was not significantly changed in the groups. *The relative mRNA expression ($2^{-\Delta CT}$) of extracellular matrix proteins COL1A1, COL3A1, DCN, LUM, LOX, and BGN in the ventricles of the mild and severe wooden breast chicken hearts. Values are presented as the average $2^{-\Delta CT}$ value of each group (N= 12 within each group) of three replicates. The genes had no significant difference between the mild and severe groups. SD is illustrated by error bars; dots represent each sample of its group. Welch's t-test was performed and did not detect any significant differences in the ECM expression between the groups (*p<.05).*

The expression level of collagen type I alpha 1 (*COL1A1*) was not significantly heightened in the severe WB samples, and collagen type 3 alpha 1 (*COL3A1*) was not significantly increased. Moreover, the relative gene expression of SLRPs, was found unchanged. Decorin (*DCN)* was not significantly downregulated in severe WB samples, and lumican (*LUM*) was not significantly increased in severe WB samples. Lysyl oxidase (*LOX*) appeared to decrease in the severe WB samples, though the reduction was not significant. Additionally, the relative gene expression of biglycan (*BGN*) seemed unchanged in both mild and severe WB samples, as shown in Figure 4.5F.

4.3.2. The gene expression of ECM enzymes and SDCs was similar in mild and severe WB samples

Additionally, fibrosis can also be detected by MMPs and TIMPs, which have a role in regulating remodelling in tissues. Dysfunction in MMPs and TIMPs activity can lead to conditions such as fibrosis (Fan et al., 2012). Syndecans are also known as regulators of fibrosis in the heart (Lunde et al., 2016).

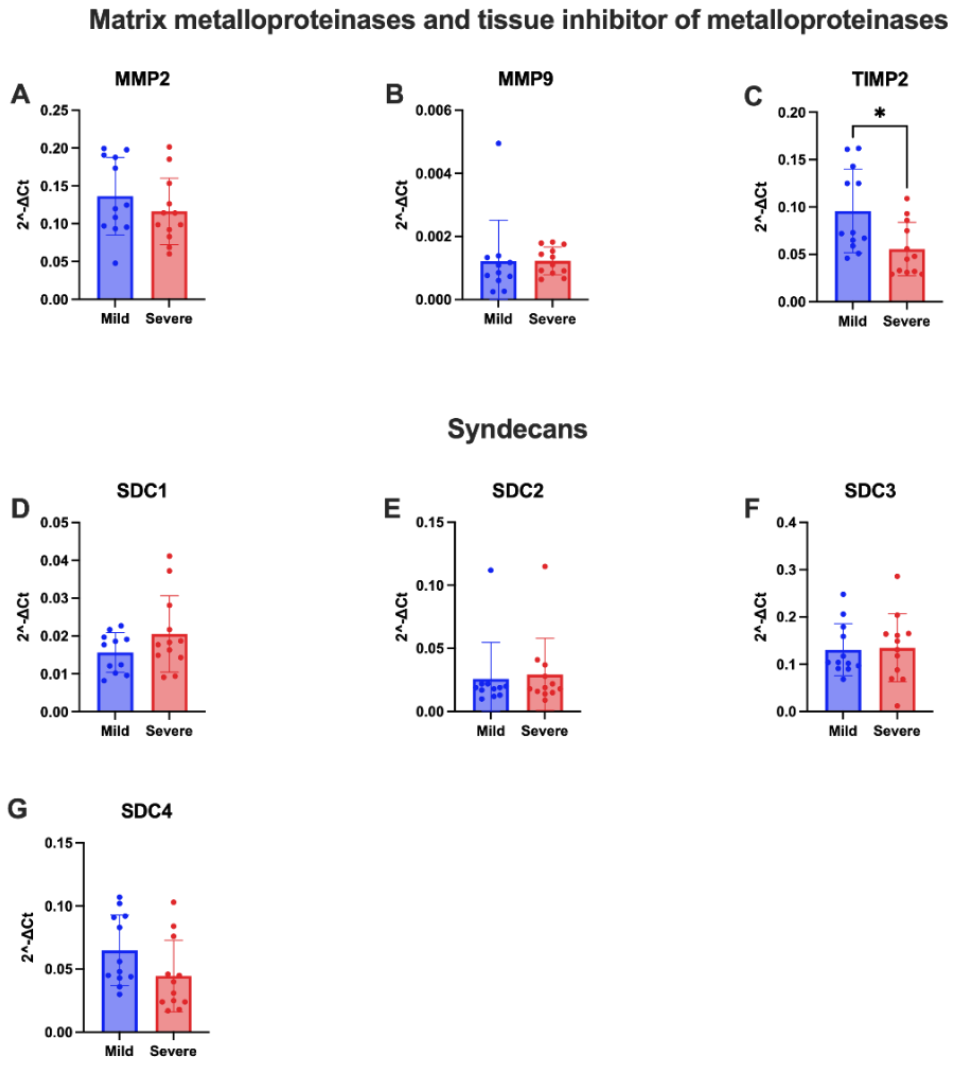

Figure 4.6. TIMP2 significantly decreased in the severe WB samples*. The average relative mRNA expression of MMP2, MMP9, TIMP2, and SDC 1-4 genes in the ventricles of mild and severe WB chicken. Values are presented as the average* $2^{-\Delta CT}$ *of each group (N=12 within each group) of three sample replicates. While MMP2 and MMP9, SDC 1-4 were not significantly different between the groups. A Welch's t-test revealed TIMP2 as a significant difference between the mild and severe groups. The asterisk shows the significant difference between the given gene's severe and mild groups (p*<0.05). Error bars illustrate SD.*

MMP2 and *MMP9* gene expression did not increase in the severe wooden breast samples. On the contrary, the relative gene expression of *TIMP2* was significantly decreased in severe WB samples presented in Figure 4.6C.

The gene expression syndecans were found unaltered. The relative gene expression of *SDC-1* was not proven to be significantly upregulated in severe samples. Moreover, the relative gene expression of *SDC-2* was also not found to be significantly increased. Furthermore, *SDC-3* did not seem to differentiate between mild and severe WB samples. On the other hand, the relative expression of *SDC-4* seemed to decrease in the severe WB samples; however, it was not significant.

4.3.3. No significant increase or decrease in the gene expression of inflammation, cardiomyocyte, myofibroblast, cytoskeleton or the transforming growth factor (TGFB) in severe WB samples

Various markers were utilised to investigate fibrosis and inflammatory responses commonly associated with WB pathology (Tong Xing et al., 2021; T. Xing et al., 2021).

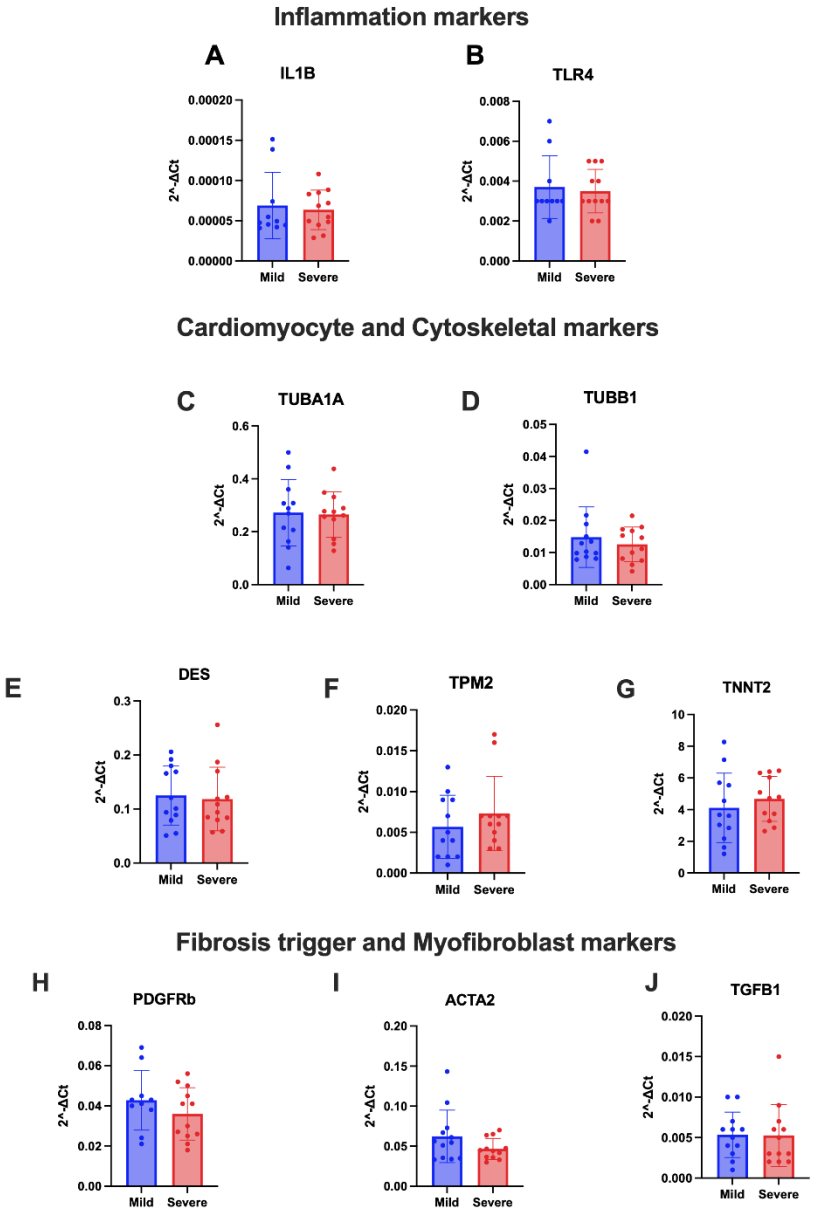

Figure 4.7. Inflammation, tubulin, cardiomyocyte, cytoskeletal, fibrosis trigger and myofibroblast markers did not change in severe WB samples. *Mean relative expression of ILB1, TLR4, TUBA1A, TUBB1, DES, TPM2, TNNT2, PDGFRb, ACTA2, and TGFB1 of three replicates of each sample between the two groups, with EEF2 as reference gene compared with mild and severe WB samples. Values in the figure are presented as the average* $2^{-\Delta CT}$ *of each group of three replicates of each sample (N=12 within each group). Unpaired Welch's t-test was performed on the data, which indicated no significant differences between the two groups. Error bars demonstrate SD.*

The gene expression inflammation markers were not increased in severe WB. Interleukin-1beta (*IL1B*) was not significantly upregulated in severe WB samples and appeared unaffected by severe WB (Figure 4.7A). Moreover, Toll-like receptor 4 (*TLR4*) relative gene expression did not exhibit alterations in the severe WB samples (Figure 4.7B) and was found not to be significantly upregulated. The relative gene expression of tubulin alpha-1A chain *(TUBA1A)* seemed unchanged in severe WB, as shown in Figure 4.7C. On the other hand, the relative gene expression of tubulin beta-1 chain *(TUBB1)* slightly decreased in the severe WB samples; however, it was found not to be significant. Desmin *(DES)* seemed unchanged in severe WB samples.

The gene expression of tropomyosin 2 (*TPM2*) seemed to increase in severe WB samples (Figure 4.7F). However, the *TPM2* was insignificant, and a slight increase of troponin T 2 *(TNNT2*), shown in Figure 4.7G, was also insignificant. The cardiac fibroblast regulator platelet-derived growth factor receptor beta *(PDGFRb)* was unchanged. Additionally, the gene expression of actin alpha 2 (*ACTA2*) showed a tendency to be downregulated. While transforming growth factor beta 1 (*TGFB1*) showed no differences in severe WB samples.

4.4. Protein expression analysis

Further, MMP2 and cardiac Troponin T (cTnT) protein expression was analysed in mild and severe WB samples.

4.4.1. MMP2 but not troponin T protein expression was consistent with gene expression

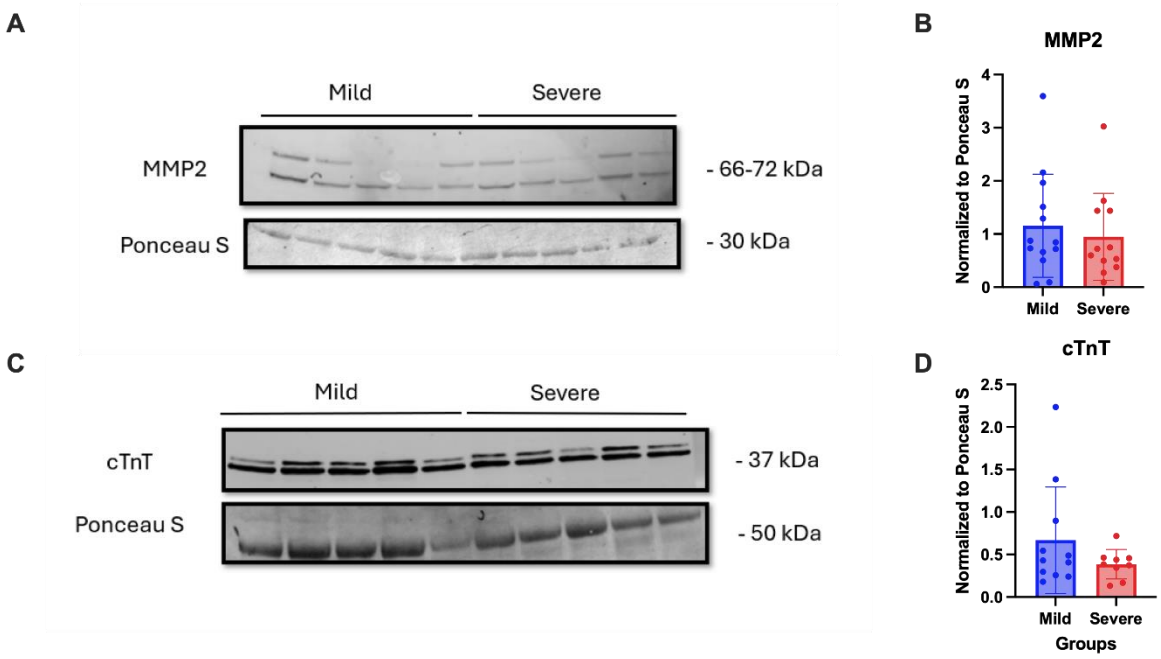

Figure 4.8. The expression of MMP2 and cTnT was not found to be significantly downregulated. *A western blot showing the protein expression of MMP2 and cTNT. Tissue lysates were subjected to Western blotting using an antibody to MMP2 and cTnT. Ponceau S was used as the loading control. As presented in A, the expression of MMP2 and cTnT relative to Ponceau S. Western blot was quantified. The relative intensity of MMP2 and cTnT was normalised to Ponceau S in each group. The graph in B represents the quantification of N= 12 mild and N= 13 severe WB. Individuals +- SD.*

The protein expression of MMP2 seemed to be decreased in the severe WB samples shown in Figures 4.8A and B, which is consistent with the relative mRNA expression presented in Figure 4.6A. However, from the strength of the bands, there is no clear distinction between the groups, and the decrease was found not to be significant.

Protein expression of cTnT seemed to decrease in the severe WB samples but was not significant. The blot presented in Figures 4.8C and D showed the opposite trend of the relative gene expression of *TNNT2* (Figure 4.7G).

4.5. RNA-Seq

The severe and mild WB samples were sequenced at Stony Brook University. The RNA-Seq was first subjected to a differential expression analysis before a gene set enrichment analysis.

4.5.1. Hierarchical clustered heatmap revealed groupings of gene expression

A differential expression analysis was performed to investigate gene expression across groups. The hierarchically clustered heatmap illustrates the differential expression analysis of the RNA-Seq data.

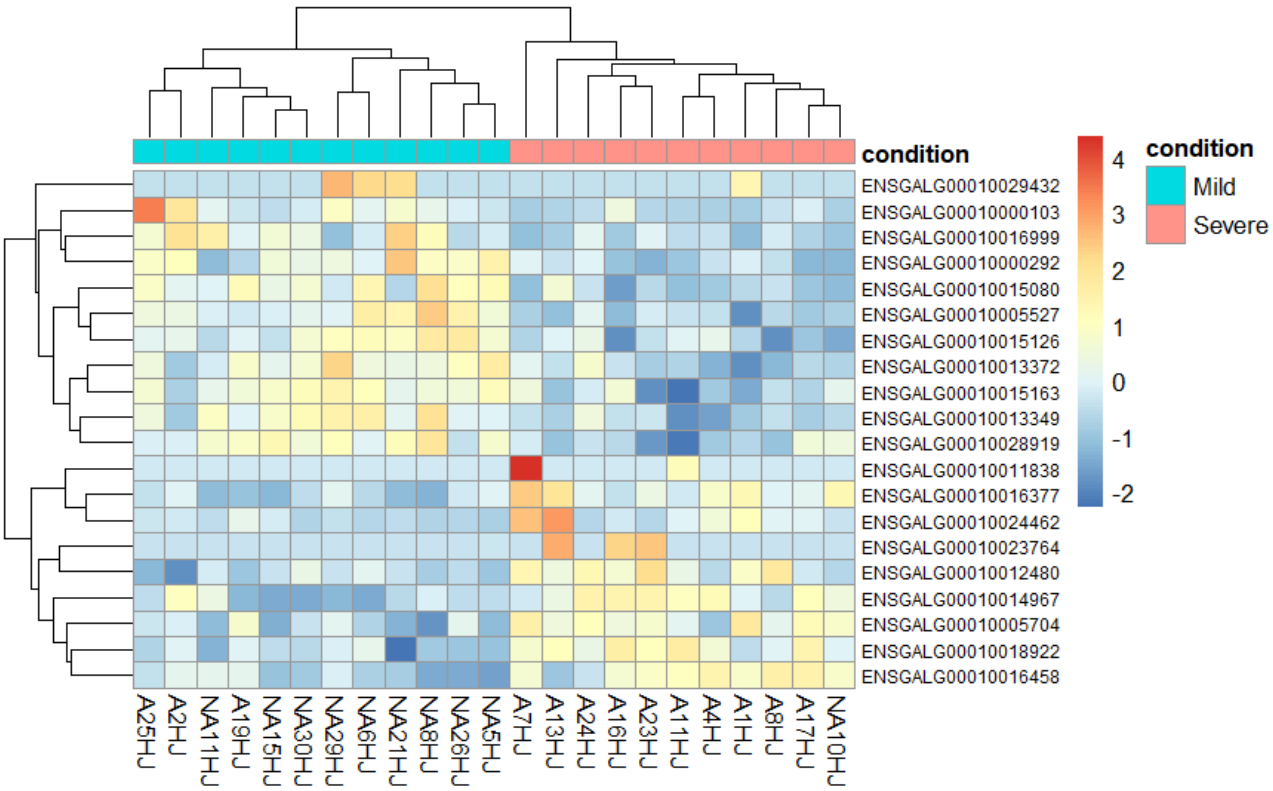

Figure 4.9. The hierarchically clustered heatmap showed different gene expressions between the groups. *Hierarchically clustered heatmap of severe versus mild WB samples. The heatmap is of z scores for the top 20 genes. The normalisation method used was the z score. Z score is calculated by taking the mean intensity of a gene from the raw intensity data of every gene and then dividing it by the SD(Cheadle et al., 2003). From the heatmap, there seems to be a pattern between the two conditions. Created in R studio.*

The gene expression levels seemed to follow a pattern in their distinctive groups. However, a few samples demonstrated different gene expression levels than the rest of their group. Figure 4.9 shows the hierarchical clustering of groups, where the samples are clustered to their respective group

4.5.2. Gene Set Enrichment Analysis

To delve into the potential biological processes influenced by WB myopathy, a gene set enrichment analysis (GSEA) was performed, utilising the gene ontology (GO) functions associated with co-expressed genes.

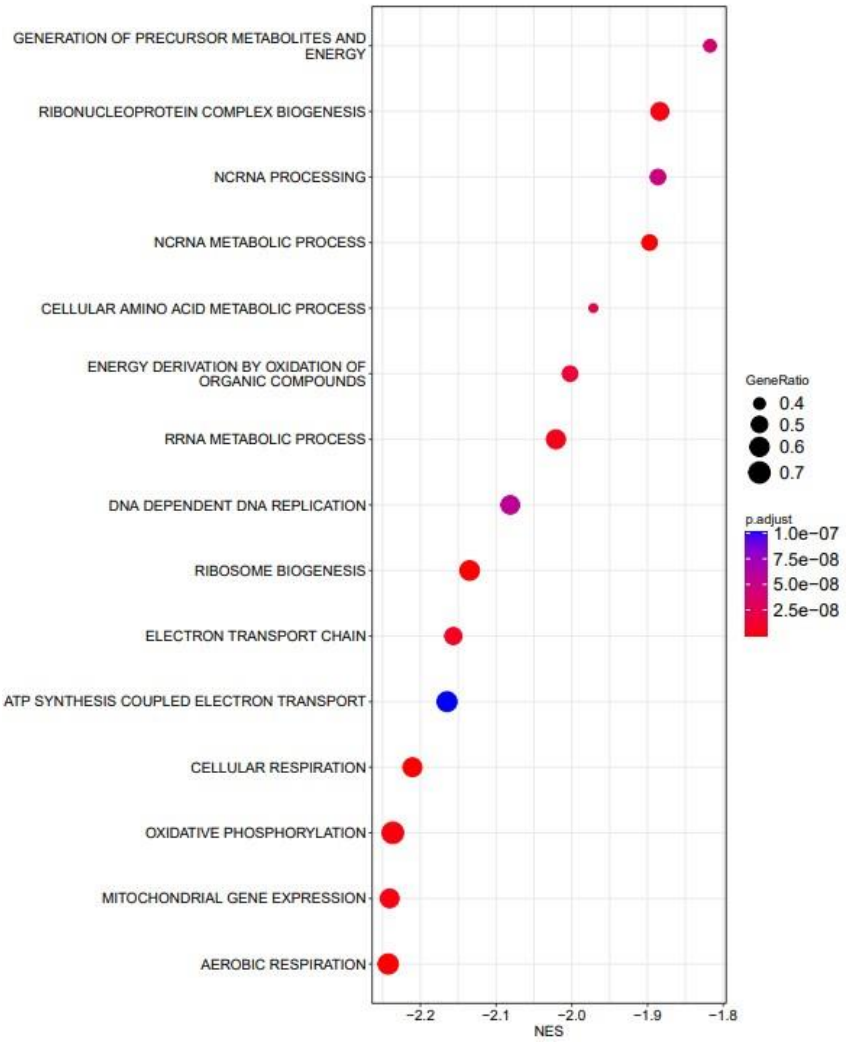

Figure 4.10. GSEA demonstrated the downregulation of critical biological processes. *Results from the Gene Set Enrichment Analysis of Gene Ontology comparing severe versus mild Ross samples. The GSEA results illustrate the GO biological processes associated with WB in mild and severe samples. The figure shows the significant top 15 downregulated GO processes for the severe WB samples. The x-axis shows the Normalized Enrichment Score (NES). The count illustrates the number of genes related to the specific GO biological process. The p-adjusted value is shown in dots in decreasing order. Provided by Dada Pisconti.*

The GSEA confirmed significant downregulation of critical metabolic processes and mitochondrial gene expression in severe WB samples compared to mild WB samples (Figure 4.10). In addition, genetic maintenance mechanisms were also significantly downregulated in severe WB samples.

4.6. The protein expression of Cytochrome C was significantly upregulated in severe WB samples

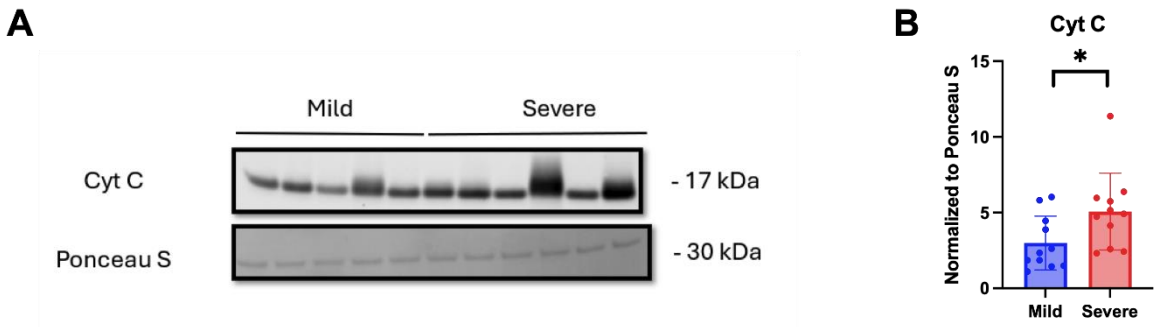

Figure 4.11. Cyt c was significantly upregulated in severe WB samples. *A western blot showing the protein expression of Cyt c. Tissue lysates were subjected to Western blotting using an antibody to Cyt c. Ponceau S was used as the loading control. As presented in A, the expression of Cyt c relative to Ponceau S. Western blot was quantified. The relative intensity of Cyt c was normalised to Ponceau S in each group. The graph in B represents the quantification of n=25. Individuals +- SD.*

Following the GSEA analysis, the protein expression of Cyt C was investigated to see if the severe WB samples exhibited mitochondrial stress. Compared to mild WB samples, the Cyt C protein expression was upregulated in severe WB samples. The bands appeared thicker and stronger in the severe WB group than in the mild group, as shown in Figure 4.11A. The upregulation of Cyt C was significant (Figure 4.11B).

4.7. Comparative analysis Hubbard and Ross

We wanted to compare the hearts of Ross 308 with the more slow-growing chicken breed Hubbard since these are less prone to develop WB. A comparative analysis was therefore performed.

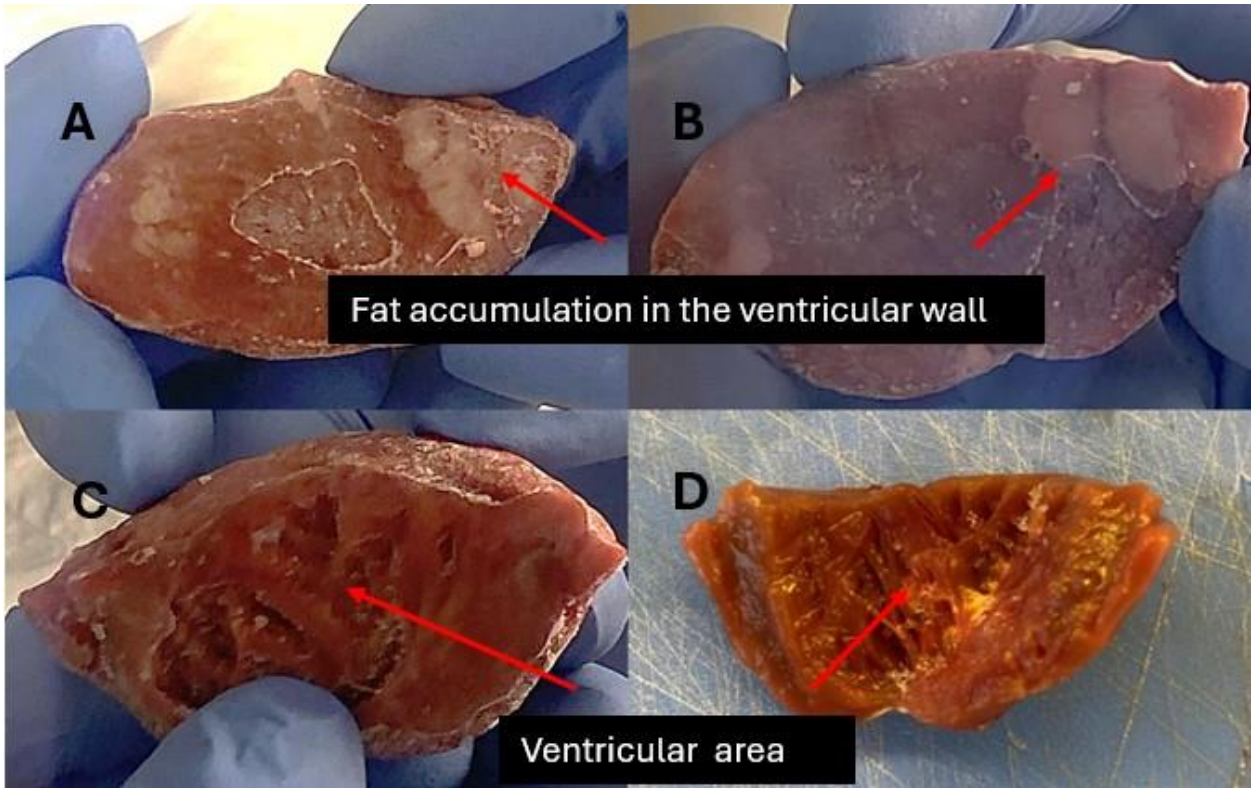

Figure 4.12. Normal Hubbard Samples had fat around the ventricles. *Mild WB Hubbard samples showed fat accumulation around the left ventricular wall and some around the right ventricle.*

Fat accumulation was observed in several mild WB samples of Hubbard, especially around the left and right ventricular walls, as shown in Figure 4.12.

4.7.1. Wooden breast's effect on Hubbard heart weight and water binding capacity

The ventricles of Hubbard hearts were weighed to observe the water binding capacity between mild and severe WB samples.

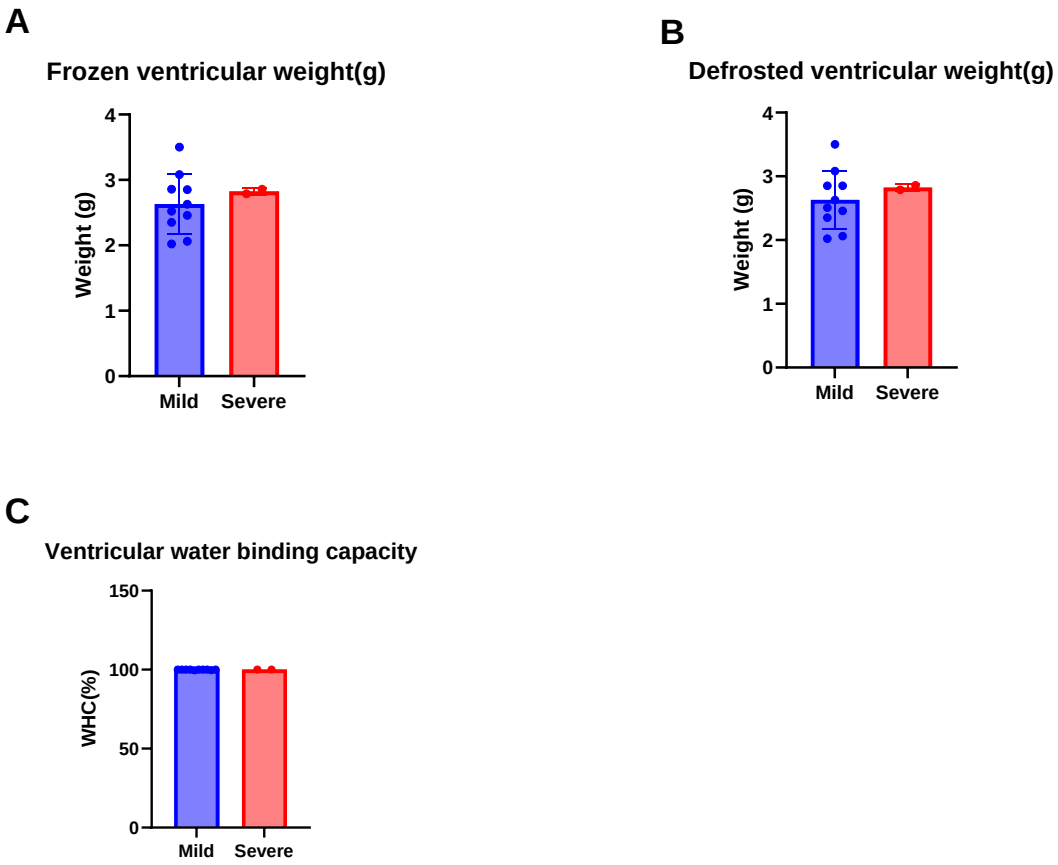

Figure 4.13. No differences between mild and severe WB Hubbard samples in their water holding capacity. *(A) The frozen weight of the ventricles seems to be different between the mild and severe samples. However, it was not proven to be significantly different, and there were only two WB samples of the Hubbard breed. The same pattern was seen in the defrosted apex weight (B) but was not significantly different between the two groups. The water binding capacity (%) indicated no significant difference between the mild and severe samples, as demonstrated in (C). An unpaired Welch's t-test was performed on the data (*p<0.05), and error bars illustrate SD. Dots represent each sample in the following group.*

The frozen ventricular weight (Figure 4.13A) showed no difference in the two groups, as did the defrosted ventricular weight (Figure 4.13B). The water binding capacity of mild and severe WB was high and was not proved significantly different (Figure 4.13C).

4.7.2. NIR spectroscopy

NIR spectroscopy was utilized to investigate the water, protein, and fat deposition in the Hubbard heart samples.

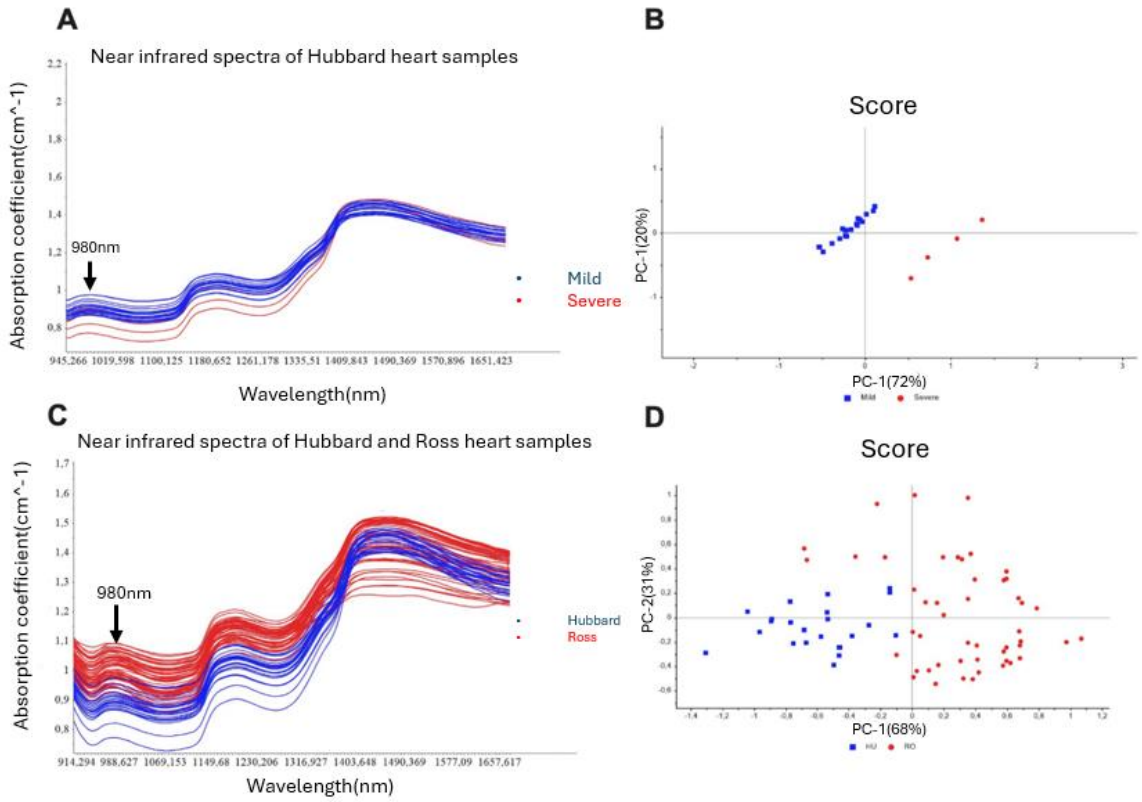

Figure 4.14.NIR spectra and PCA analysis of Hubbard samples showed differences between the chicken breeds. *(A) Near-infrared spectra show the raw absorption of mild and severe WB samples. The x-axis demonstrates the wavelength (nm) at which the samples' light absorption occurs. The severe and mild WB samples showed no differences in light absorption. The arrow shows the water peak at 980 nm. (B) Principal Component Analysis (PCA) of Hubbard heart samples, the mild and severe WB samples did differentiate, and there is a clear grouping of samples. (C) Raw absorption spectra of Ross and Hubbard samples were obtained using NIR spectroscopy. There is a distinction between the two chicken breeds in the absorption of light capacity. The x-axis demonstrates the wavelength (nm), while the y-axis shows light absorption (cm^{-1}). (D) Principal Component Analysis (PCA) of Ross and Hubbard WB samples. From the PCA, the breeds seem quite different in terms of chemical and physical properties.*

The results indicate a physical difference between severe and mild WB Hubbard samples (Figure 4.14A-B). However, only two severe WB samples were used in the analysis, so it is difficult to draw conclusions based on these few samples. The PCA analysis indicated differences among the severe and mild WB samples. The sample grouping of severe and mild WB samples is shown in Figure 4.14B.

The results of the NIR spectroscopy indicate that the light absorption in Ross heart samples is higher than that of Hubbard heart samples (Figure 4.14C). The breeds demonstrate a distinction from the raw absorption spectra, and at 980 nm. The heart tissue of Ross and Hubbard seemed to differentiate. It was grouped in the PCA analysis, which indicated differences in their chemical/physical composition in heart tissue, as presented in Figure 4.14D.

4.7.3. Collagen and fat deposition in Hubbard samples

The collagen deposition in the ventricles of Hubbard was investigated.

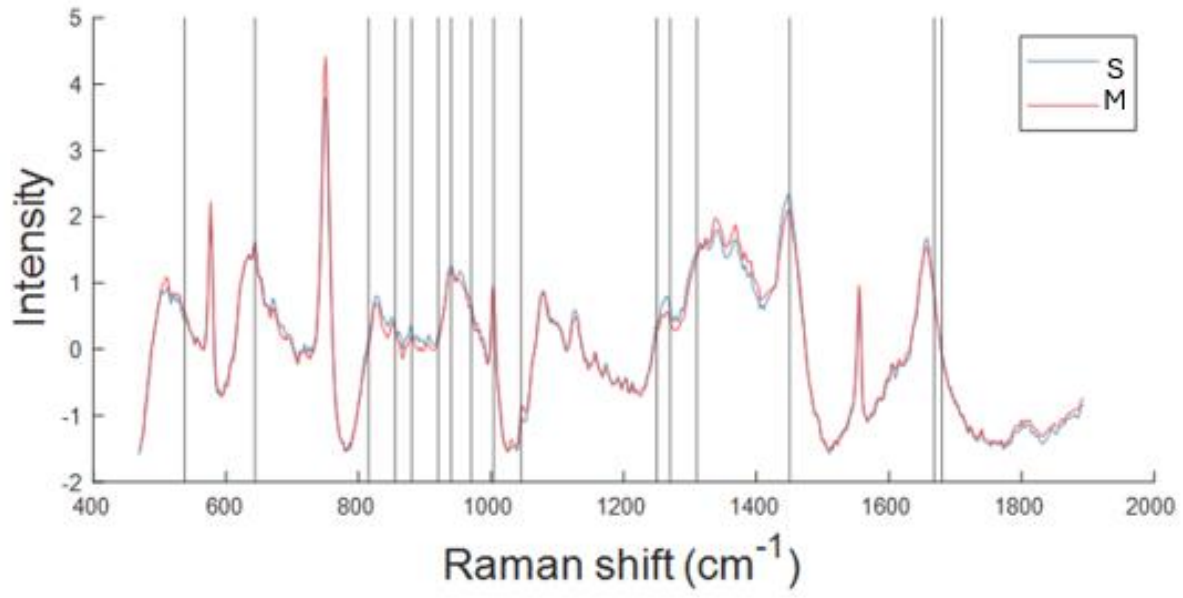

Figure 4.15. There were no signs of collagen accumulation in Hubbard WB samples. *The average Raman spectra of Hubbard samples did not indicate any changes in collagen in the ventricles of Hubbard heart samples. The Raman spectra were baseline corrected and SNV normalised. The ratios 827/854, 919/936, 1657/1678, and 1315/1340; are peaks where collagen can be measured.*

The results show a lack of heightened collagen accumulation in severe WB samples compared with mild WB samples, as depicted in Figure 4.15. Disparities in the fluorescence intensity observed among samples are a result of autofluorescence.

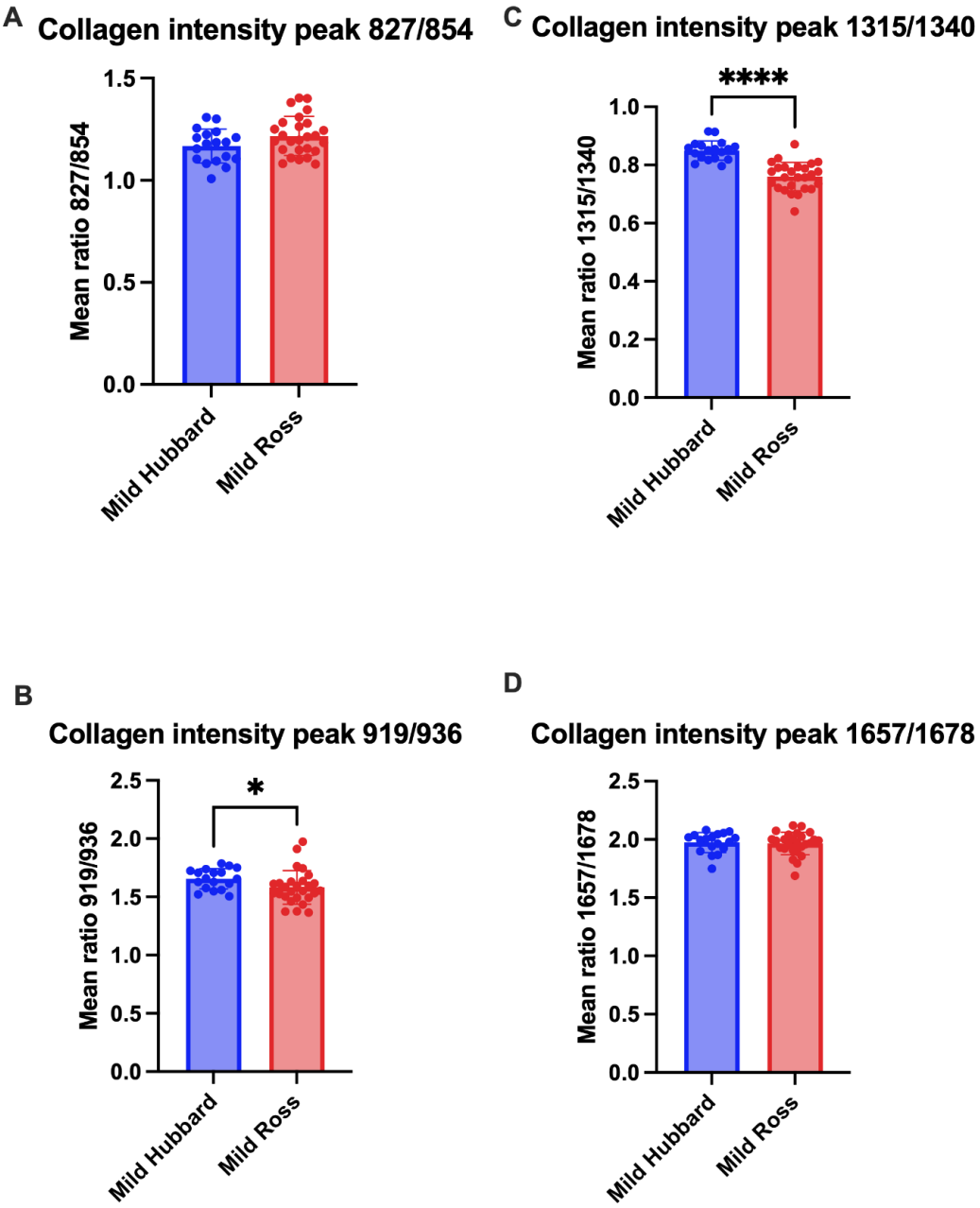

Figure 4.16. Collagen intensity peaks 919/936 and 1315/1340 were significantly higher in Hubbard. *The mean collagen peak intensity ratios from Raman Spectroscopy were performed on Hubbard samples. A-D shows the collagen peak ratios (A)827/854, (B)919/936, (C) 1315/1340, and (D)1657/1678, which indicate the sample's collagen composition. An unpaired Welch's t-test was performed, and the results ratios of 919/936 and 1315/1340 were found significant. The error bars illustrate the SD.*

As demonstrated in Figure 4.16 A-D the collagen deposition in mild WB Hubbard samples was found to be significantly higher than in mild Ross samples at intensity peaks 919/936 and 1315/1340.

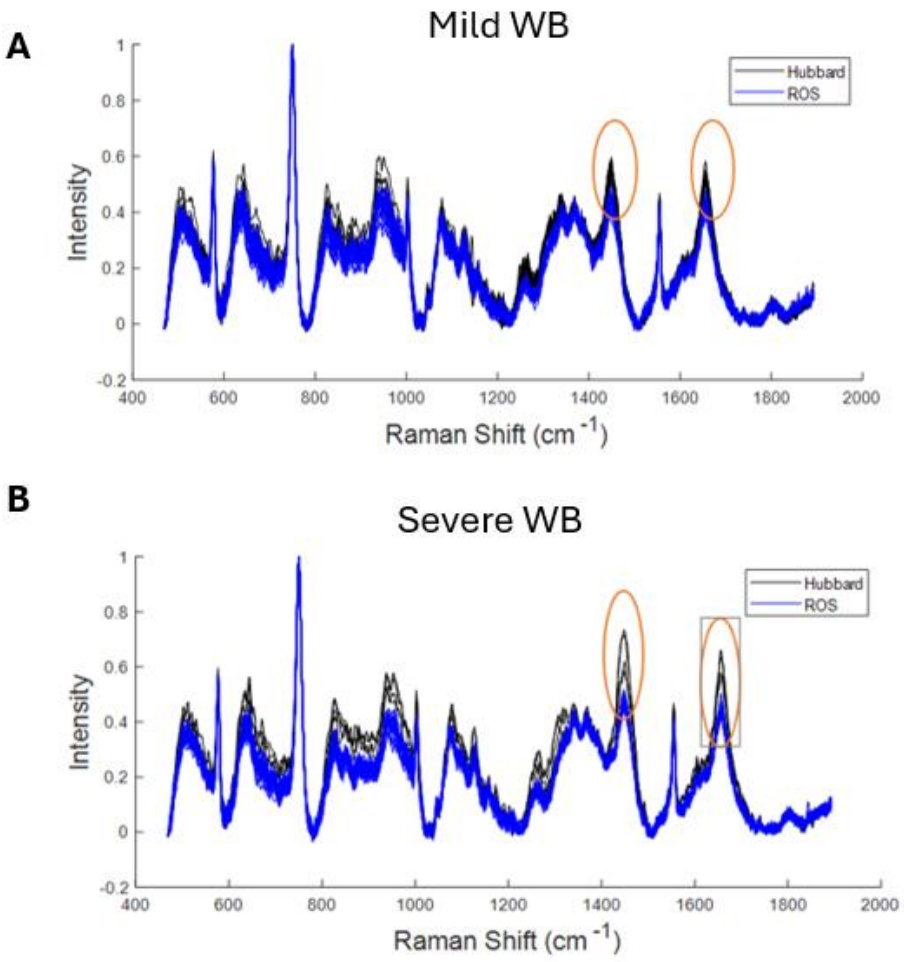

Figure 4.17. Mild and severe samples of Hubbard showed higher fat accumulation compared to Ross. *The circles show the peaks where fat can be measured. Both mild and severe samples of Hubbard demonstrated higher fat accumulation than Ross in both groups. The Raman spectra were baseline corrected and sapphire normalised.*

Hubbard heart samples had higher fat signals than Ross in severe and mild WB samples. The Raman analysis indicated that the hearts of Hubbard chickens contained more fat than Ross's heart samples, as presented in Figure 4.17A-B.

4.7.4. SimplyBlue protein expression

SimblyBlue staining was performed to investigate the difference in protein expression between the two breeds.

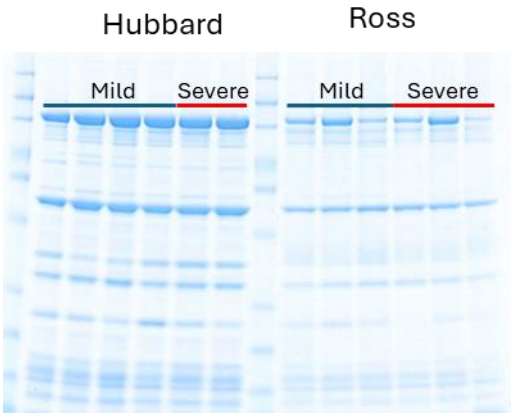

Figure 4.18. The protein expression of Hubbard and Ross showed differences. *SimplyBlue Protein expression of the two chicken breeds is mild and severe WB samples. The severe samples are marked with the red bar and the mild samples with the blue bar. The Hubbard samples had more protein bands than the Ross samples, and the overall protein expression was stronger in Hubbard.*

Protein expression was higher overall in the Hubbard samples than in the Ross samples. Hubbard's mild and severe samples did not indicate much difference in protein expression. Conversely, differences between the mild and severe groups were observed within the Ross samples (Figure 4.18).

4.7.5. MMP2 expression was higher in mild Ross samples

The western blot result of the Ross samples was compared with Hubbard samples to observe if the gene expression was similar across chicken breeds.

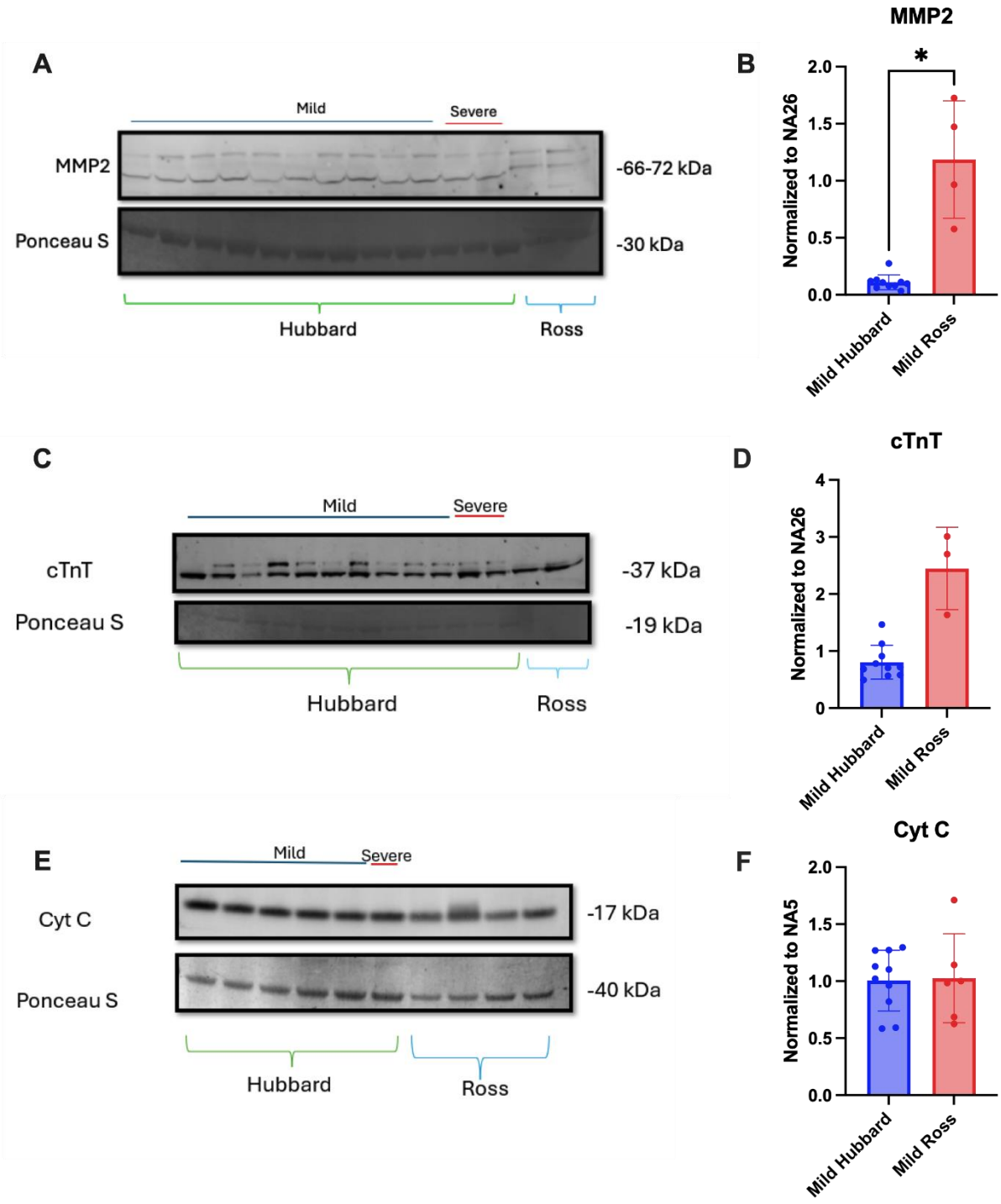

Figure 4.19. Protein expression of Cyt C and cTnT was similar in Hubbard and Ross 308 mild samples, whereas MMP2 expression was lower in Hubbard. *A western blot showing MMP2, cTnT, and Cyt C. Tissue lysates' protein expression was subjected to Western blotting using an antibody to MMP2, cTnT, and Cyt C. Ponceau S as a loading control. Expression of,*

MMP2, cTnT and Cyt c relative to Ponceau S. Western blot, as presented in A, C, E, was quantified. The graph represents the quantification of n=10 Hubbard Individuals +—SD and n=3-5 Ross individuals +- SD. Outliers of Ross were removed.

The bands showed lower MMP2 expression in mild WB Hubbard samples compared to mild WB Ross samples. However, the protein expression of MMP2 was significantly upregulated in the mild WB Ross samples, as shown in Figure 4.19B.

Figure 4.19C shows the protein bands from the western blotting with cTnT of Hubbard samples. The protein expression of cTnT was lower in mild WB Hubbard samples than mild WB Ross samples. The increase in protein expression in mild WB Ross samples was not proved significant.

Western blotting analysis of Cyt c in Hubbard revealed a consistent expression level across both mild and severe samples, with no visible discrepancy between the two groups, as seen in Figure 4.19E. The mild Hubbard and Ross samples showed similar expressions of Cyt c, as shown in Figure 4.19F.

5. Discussion

5.1. Wooden breast-affected broiler chickens and the susceptibility to cardiac fibrosis

In the present study, we investigated molecular markers for cardiac fibrosis in wooden breast-affected chickens since skeletal muscle fibrosis is a well-known pathology of WB. The hypothesis of cardiac fibrosis in WB-affected chicken was built on pathology found in DMD, where the patients develop skeletal fibrosis and then develop severe cardiomyopathies at a later stage (van Westering et al., 2015). NIR and Raman spectroscopic analysis did not reveal major differences between mild and severe WB groups. NIR analysis is used to classify WB skeletal muscle, where a shift in water-binding and reduced protein content is observed (Wold et al., 2019). From the frozen and thawed ventricular weight analysis, mild and severe WB samples in Ross appeared to have good water-holding capacities, as no significant alterations were observed in either group. This finding may suggest that the severe WB samples have no fibrosis in their heart tissue, as fibrotic tissues tend to hold water poorer than non-fibrotic tissues (Soglia et al., 2016). The impairment of water-holding capability is typical in breast fillets of WB broiler chickens. It is due to the degeneration of muscle fibres, with fibrosis and lipidosis supplemented since most water is in myofibrils. Moreover, chemical composition changes can also play an essential role in reducing WHC (Soglia et al., 2016). WB-affected chickens have demonstrated poor WHC (Zhang et al., 2020). The WHC characteristic of WB was not observed in the heart tissue, indicating that the heart of WB-affected chickens may not be affected by fibrosis or myofiber degeneration and reduced protein content as seen in skeletal muscle (Pejšková et al., 2023). However, it is important to outline that no histology on the cardiac tissue was included in this study. Further analysis with staining of cardiac structure and cardiomyocytes should be performed to support this suggestion of minor cardiomyocyte and myofiber degeneration in WB.

Raman's spectroscopy analysis showed that Ross's heart tissue showed no signs of increased collagen accumulation in the ECM, further supporting no extensive remodelling of ECM as seen in fibrosis (Li et al., 2018). The ECM shows no collagen accumulation due to fibrosis in the severe WB samples. The variances seen in the Raman spectra between the samples in intensity are most likely due to autofluorescence. Molecules found in cells can become fluorescent when stimulated by UV/Vis radiation of appropriate wavelength. Especially in the ECM, the autofluorescence is higher than the cellular components due to collagen and elastin's high quantum yield (Monici, 2005). Quantitative gene expression analysis of

COL1A1 and *COL3A1* supported the observations from the Raman spectroscopy analysis of the Ross samples. However, the gene expression analysis did show a slight increase in *COL1A1* and *COL3A1* of the severe WB group, however it was not significant.

In this study, we did not observe increased collagen deposition in the severe WB samples, which indicates no remodelling of the ECM, a characteristic of fibrosis and was also found in the skeletal muscle in severe WB (Pejšková et al., 2023). This finding also supports the unchanged SLRPs *LUM, BGN* and *DCN* gene expression, which often cross-link with fibrillar collagen. SLRPs are collagen fibril regulators that regulate collagen crosslinking and stiffness in the ECM and have been shown to be involved in the development of cardiac fibrosis and ECM remodelling (Christensen et al., 2019; Mohammadzadeh et al., 2019). Typically, *DCN* and *LUM* are increased in muscular dystrophies (Pejšková et al., 2023; Velleman, 2015; Velleman & Song, 2017; Xing et al., 2020; Zanotti et al., 2005). The same upregulation was not observed in the hearts of severe WB broiler, which suggests that the heart tissue is non-fibrotic. Moreover, *BGN* was also unaffected in the heart samples, a factor described as an inflammatory factor found in fibrotic tissues (Schaefer et al., 2005). This finding is supported as in the skeletal muscle of severe WB, no alterations in the *BGN* expression were found. *BGN* has been suggested not to be participating in the responses to inflammation in WB (Pejšková et al., 2023).

An imbalance in the synthesis and degradation of ECM components regulated by MMPs and their inhibitors TIMP is observed in fibrosis (Alameddine & Morgan, 2016). Furthermore, one regulator of fibrosis *TIMP2* was significantly decreased in severe WB samples. The reduced expression of *TIMP2* has been correlated with pronounced myocardial interstitial fibrosis and disruption of the ECM in mice undergoing pressure overload (Kandalam et al., 2011). However, the function of *TIMP2* and its effect on cardiovascular cells and tissue remodelling is poorly understood (Ngu et al., 2014). Additionally, the lack of *TIMP2* can cause a reduction of collagen cross-linking protein *LOX*. No difference in *LOX* expression between the two groups was obtained in this study. However, the impact of *TIMP2* on cardiac fibrosis is governed by the injury type or stimulus (Fan & Kassiri, 2021).

TIMP2 can inhibit the activity of *MMP2* but also suppress its expression (Ngu et al., 2014). In the severe WB samples, the *MMP2* gene and protein expression seemed reduced. A study on mice demonstrated that *MMP2* deficiency affected cardiac function (Wang et al., 2015). Nevertheless, we could not detect TIMP1 and TIMP2 protein expression by using western

blot. The use of TIMPS and MMPs as biomarkers for several cardiac diseases has conflicting results (Fan et al., 2014; Li et al., 2018). The syndecan family is involved in cardiac fibrosis (Lunde et al., 2016). Based on the results, *SDC-2* and *SDC-3* gene expression were unchanged between normal and severe WB samples, while *SDC-1* and *SDC-4* exhibited alterations in their gene expression. However, the upregulation of *SDC-1* and the downregulation of *SDC-4* were not significant. SDC-1 expression is suggested to increase by tissue injuries, inflammatory regulations, and reparative responses(Lunde et al., 2016). This study showed no difference in the groups' inflammation markers, such as *TLR4* and *IL1B*, at mRNA levels. Furthermore, SDC-4 has been suggested to be upregulated by IL1B (Strand et al., 2013). The gene expression of *SDC-4* and *IL1B* proposes that the severe WB hearts do not exhibit any signs of inflammation. However, in the skeletal muscle of these broilers, the SDC expression was found to be important and increased (Pejšková et al., 2023).

Moreover, reduced *SDC-1* expression induces the activity of *MMP2* and *MMP9*, leading to collagen disorganization (Lunde et al., 2016). For these reasons, it might be suggested that the WB-affected broiler chickens have quite healthy hearts since the regulation of *SDC-1* is unaffected in their heart. Also, the downregulation of *SDC-4* has been observed to reduce myocardial stiffness due to decreased collagen cross-linking (Herum et al., 2015). SDC-4 is known as a regulator of cardiac fibrosis (Herum et al., 2020). Therefore, a lack of *SDC-4* in severe WB samples could contribute to the progression or development of cardiac fibrosis (Lunde et al., 2016). However, the decrease of *SDC-4* was not significant. If the decrease of *SDC-4* had been substantial, the collagen deposition or cross-linking would have been attenuated, according to other studies (Herum et al., 2013). This was not implied by the qPCR, NIR and Raman analyses of the heart samples.

Cytoskeletal and muscle fibre markers did not exhibit alterations from gene expression and were not detectable in the protein expression analysis. *TUBB1, TUBA1A, DES* expression was not increased in the severe WB samples. Microtubules have been suggested to be a marker for the development of heart failure (Gürtl et al., 2009). A study from (Heling et al., 2000) demonstrated that tubulins and *DES* increased mRNA and protein levels in human heart failure. This might suggest that the hearts are not undergoing heart failure as this is a compensatory mechanism typical in heart failure (Hein et al., 2000). In contrast, an unaltered microtubule network could indicate another phase of remodelling in the structure of the cell (Belmadani et al., 2002).

Apart from this, cTnT protein expression levels were also found to be unchanged. A study from (Mesnard-Rouiller et al., 1997) concluded that cTnT mRNA and protein expression was found in all failing ventricles and may not be considered as characteristic of failing human left ventricles. Another study also demonstrated elevated cTnT levels in patients with skeletal myopathies and suggested a cross-reaction with isoforms of skeletal muscle troponin when using immunoassay (Schmid et al., 2018). This might suggest that cTnT is unsuited as a biomarker for cardiomyopathies in muscular dystrophy disease.

Although there were minor differences in ECM markers of fibrosis, the data in this study indicated mitochondrial dysfunction in the WB-affected broiler's hearts. The GSEA of the RNA-Seq data found alterations in the mitochondrial function, where mitochondrial gene expression, oxidative phosphorylation and ATP electron transport chain were significantly downregulated in the severe samples. The downregulation of oxidative phosphorylation in the mitochondria may also indicate the beginning of a myocardial infarction, where the cardiomyocytes shift from oxidative phosphorylation to anaerobic glycolysis due to a lack of oxygen and nutrients (Bisaccia et al., 2021). Nonetheless, ATP production is crucial for the transfer system to function correctly (Bisaccia et al., 2021). Energy deficit is a crucial contributor to both cardiac and skeletal myopathy development. Moreover, the heart is a very energy-demanding organ and needs ATP continually for muscle contraction and relaxation. In heart failure, various bioenergetic factors are changed, mitochondrial ATP production being one of them (Rosca & Hoppel, 2013).

Based on these findings, it can be indicated that the hearts of severely wooden breast-affected broiler chickens might be in the progression of heart failure or other cardiomyopathies. On the other hand, mitochondrial dysfunction and cardiac fibrosis are often seen together as their mechanisms coincide (X. Li et al., 2020). In addition to this, the Cyt c expression was found to increase in severe WB samples. Cyt c is released when the mitochondrial permeability transition pore opens due to dysfunction of the mitochondrial respiratory chain. Moreover, Cyt c triggers cell apoptosis that subsequently stages the progression of heart failure (Liu et al., 2022). A limiting factor in our study may be the age of the broilers, who were only 36 days old when slaughtered. Cardiomyopathy may be more prominent if the broilers were slaughtered at a later stage, and it is unsure how early in the pathogenesis the broiler chickens are. In DMD, cardiac disease is gradual, and eventually leads to dysfunction of the ventricles, and dilation (Mazur et al., 2012). At later stages in the disease, the patients exhibit

hypertrophy and atrophy of the cardiomyocytes, in addition to fibrosis (Frankel & Rosser, 1976; Moriuchi et al., 1993).

5.2. Hubbard and Ross hearts differ in protein pattern and fat compositions, which might be related to cardiac health

In mild and severe samples, Hubbard and Ross's water holding capacity was unaffected. However, the Ross heart samples absorbed light better than the Hubbard samples, which can indicate different cell structures. Since NIR can penetrate deep into biological soft tissues, the absorption varies on the water, fat, and collagen ratio (Tsai et al., 2001). Hubbard samples had lower light absorption in the ventricular area, most likely due to finer cell structure. Hubbard's mild WB samples showed higher fat deposition than Ross's from examining the heart samples before dissecting; however, the NIR analysis did not confirm this finding. If Hubbard had a higher fat accumulation in their ventricular wall, it would be more obvious in the NIR spectra as light absorption would be altered. On the other hand, fat accumulation was clearly seen in the ventricular wall visually (Fig 4.12), which was not where the laser measured the composition. This could explain the discrepancy in fat measurement by NIR analysis and visual inspection of fat accumulation morphology. Usually, fat infiltration in the right ventricular muscle area can be associated with inherited myopathies such as DMD.

In contrast, the Raman analysis demonstrated different compositions of the heart tissue between the two breeds. The signal collected from Raman spectroscopy is more consistent because it is less affected by water than other infrared analyses (Auer & Skinner, 2008). Hubbard heart samples showed higher peaks than Ross and generally had higher fat signals in mild and severe WB samples, supporting the visual observation of fat accumulations in Hubbard.

Conversely, fat infiltration in the heart can also be seen in healthy individuals as an involution of ageing (Tansey et al., 2005). A study by Tansey et al., 2005 revealed that fatty infiltration can be mistaken for a myocardial disease called arrhythmogenic right ventricular myocardium (ARVC), where fat and fibrous tissue replace the right ventricular myocardium. Nonetheless, without exhibiting fibrosis, Burke et al., 1998 concluded that fat infiltration is commonly found in the right ventricle, and ARVC can only be diagnosed with detectable fibrosis (Burke et al., 1998).

The mild Hubbard samples also demonstrated higher collagen deposition than Ross in two intensity peaks specific to collagen, as shown in Figure 4.16. This finding may suggest that

the Hubbard hearts have higher collagen deposition in the ECM compared to Ross. Accumulation of collagen is often associated with fibrosis and other cardiac diseases (de Jong et al., 2012). However, no other fibrotic markers, such as MMP2 indicated that the Hubbard hearts have increased collagen deposition in the ECM. Based on the result, the mild Hubbard hearts may be in the progression of ARVC or heart failure. However, more analyses need to be done to conclude the health status of these slow-growing broilers, and the differences between Hubbard and Ross in their fat and collagen deposition may be normal.

Ross and Hubbard protein expression patterns differed, which might be due to physiological processes, and MMP2 expression was relatively higher in mild WB Ross samples than in mild WB Hubbard samples. The MMP2 levels in Ross heart samples were significantly higher, possibly due to several factors or conditions in the heart. However, induced expression is normally found in a failing heart (Bergman et al., 2007). A study by Bergman et al., 2007 demonstrated that MMP2 activity leads to heart failure phenotype, which also leads to mitochondrial disruption supported by our study. A comparative study using fast-growing *libitum* fed broilers and slow-growing feed-restricted broilers demonstrated heightened MMP2 activity in the blood plasma of fast-growing broilers with the pathogenesis of heart failure and ascites (Olkowski et al., 2003).

As mentioned by Olkowski et al., 2003, the fast-growing broiler might exhibit higher MMP2 activity than the slower-growing broilers due to rapid growth factors. MMP synthesis and activation have been revealed to be controlled by different hormones, cytokines, and growth factors (Rooprai et al., 2000; Tyagi et al., 1995). For this reason, the MMP activity might be induced in Ross.

5.3. Methodical issues

Given that no studies have been done on the hearts of wooden breast-affected chickens, there were no well-known methods and biomarkers compatible with studying fibrosis in poultry hearts. Finding a housekeeping protein such as GAPDH, vinculin, and α-tubulin was difficult since the expression was not the same across mild and severe samples, and GAPDH was unable to be detected using western blot even though it has worked at Ullevaal. The normalisation of the western blot in this study was a hassle, as no housekeeping protein worked as expected. Therefore, due to lack of time, Ponceau S was done after blotting. This made the total protein difficult to visualise as Ponceau S works better before blotting, and only a few bands were shown after staining. Moreover, since the molecular mechanism in

chickens' hearts is not well studied, choosing biomarkers to detect fibrosis was difficult as many probes are not target-specific for chickens.

For the comparative analysis, the western blot was normalised using Ponceau S and then normalised again using a mild sample NA26. Due to lack of time the layout for the comparative analysis was not optimal, and only a few Ross samples were used. Therefore, the result of the statistical analysis from the western blot analysis of Hubbard and Ross can be incorrect. Besides, the spectroscopy results could be misleading as only one part of the ventricle, and a restrictive area of the whole heart were measured in our analysis. This can lead to wrong conclusions regarding water, protein, and fat deposition.

6. Conclusion

Collectively, the findings in our study imply that the heart muscle of wooden breast-affected chickens may experience heart failure due to mitochondrial dysfunction despite not developing fibrosis in their heart muscles. Signs of mitochondrial dysfunction were observed, e.g. increased Cyt c expression and MMP2 protein expression, downregulation of mitochondrial gene expression, oxidative phosphorylation and ATP electron coupled electron transport chain. Based on the western blot and spectroscopy results, Hubbard's heart did not intuitively seem healthier than Ross's. However, the two breeds showed obvious differences in cell structure and protein expression. Hubbard's heart demonstrated fat infiltration, which may be health-related problems and possible collagen accumulation, while the hearts of Ross showed mitochondrial dysfunction. Furthermore, more analyses need to be done to determine the health status of Hubbard hearts. This study found only mitochondrial alterations in Ross's WB-affected hearts.

7. Further research

Since no earlier studies have investigated the molecular mechanisms behind wooden breast-affected chicken hearts, the present study can help future studies. Studying mitochondrial dysfunction can provide a more comprehensive overview of broiler chickens' heart health. Moreover, since Nortura AS is now changing from Ross 308 to a more slow-growing breed, a comparative study should also be done using older broilers and other breeds to attain an overview of the health of across breeds.

8. References

Alameddine, H. S., & Morgan, J. E. (2016). Matrix Metalloproteinases and Tissue Inhibitor of Metalloproteinases in Inflammation and Fibrosis of Skeletal Muscles. *Journal of Neuromuscular Diseases*, *3*, 455-473. https://doi.org/10.3233/JND-160183

Andenæs, K. (2022). *Translational cardiac research: Importance of the matrix molecules fibromodulin and lumican in left ventricular pressure overload* [PhD, University of Oslo, Norway].

Auer, B. M., & Skinner, J. L. (2008). IR and Raman spectra of liquid water: Theory and interpretation. *The Journal of Chemical Physics*, *128*(22). https://doi.org/10.1063/1.2925258

Azevedo, P. S., Polegato, B. F., Minicucci, M. F., Paiva, S. A. R., & Zornoff, L. A. M. (2016). Cardiac Remodeling: Concepts, Clinical Impact, Pathophysiological Mechanisms and Pharmacologic Treatment. *Arquivos Brasileiros De Cardiologia*, *106*(1), 62-69. https://doi.org/10.5935/abc.20160005

Belmadani, S., Poüs, C., Ventura-Clapier, R., Fischmeister, R., & Méry, P.-F. (2002). Post-translational modifications of cardiac tubulin during chronic heart failure in the rat. *Molecular and Cellular Biochemistry*, *237*(1), 39-46. https://doi.org/10.1023/A:1016554104209

Bergman, M. R., Teerlink, J. R., Mahimkar, R., Li, L., Zhu, B.-Q., Nguyen, A., Dahi, S., Karliner, J. S., & Lovett, D. H. (2007). Cardiac matrix metalloproteinase-2 expression independently induces marked ventricular remodeling and systolic dysfunction. *American Journal of Physiology-Heart and Circulatory Physiology*, *292*(4), H1847-H1860. https://doi.org/10.1152/ajpheart.00434.2006

Bisaccia, G., Ricci, F., Gallina, S., Di Baldassarre, A., & Ghinassi, B. (2021). Mitochondrial Dysfunction and Heart Disease: Critical Appraisal of an Overlooked Association. *International Journal of Molecular Sciences*, *22*(2), 614. https://www.mdpi.com/1422-0067/22/2/614

Brower, G. L., Gardner, J. D., Forman, M. F., Murray, D. B., Voloshenyuk, T., Levick, S. P., & Janicki, J. S. (2006). The relationship between myocardial extracellular matrix remodeling and ventricular function☆. *European Journal of Cardio-Thoracic Surgery*, *30*(4), 604-610. https://doi.org/10.1016/j.ejcts.2006.07.006

Burke, A. P., Farb, A., Tashko, G., & Virmani, R. (1998). Arrhythmogenic Right Ventricular Cardiomyopathy and Fatty Replacement of the Right Ventricular Myocardium. *Circulation*, *97*(16), 1571-1580. https://doi.org/doi:10.1161/01.CIR.97.16.1571

Burnette, W. N. (2009). Western Blotting: Remembrance of Things Past. In B. T. Kurien & R. H. Scofield (Eds.), *Protein Blotting and Detection: Methods and Protocols* (pp. 5-8). Humana Press. https://doi.org/10.1007/978-1-59745-542-8_2

Cheadle, C., Vawter, M. P., Freed, W. J., & Becker, K. G. (2003). Analysis of Microarray Data Using Z Score Transformation. *The Journal of Molecular Diagnostics*, *5*(2), 73-81. https://doi.org/https://doi.org/10.1016/S1525-1578(10)60455-2

Choi, J., Shakeri, M., Kim, W. K., Kong, B., Bowker, B., & Zhuang, H. (2024). Water properties in intact wooden breast fillets during refrigerated storage. *Poultry Science*, *103*(3), 103464. https://doi.org/https://doi.org/10.1016/j.psj.2024.103464

Christensen, G., Herum, K. M., & Lunde, I. G. (2019). Sweet, yet underappreciated: Proteoglycans and extracellular matrix remodeling in heart disease. *Matrix Biology*, *75-76*, 286-299. https://doi.org/https://doi.org/10.1016/j.matbio.2018.01.001

D'Armiento, J. (2002). Matrix Metalloproteinase Disruption of the Extracellular Matrix and Cardiac Dysfunction. *Trends in Cardiovascular Medicine*, *12*(3), 97-101. https://doi.org/https://doi.org/10.1016/S1050-1738(01)00160-8

de Jong, S., van Veen, T. A. B., de Bakker, J. M. T., & van Rijen, H. V. M. (2012). Monitoring cardiac fibrosis: a technical challenge. *Netherlands Heart Journal*, *20*(1), 44-48. https://doi.org/10.1007/s12471-011-0226-x

Dixon, L. M. (2020). Slow and steady wins the race: The behaviour and welfare of commercial faster growing broiler breeds compared to a commercial slower growing breed. *Plos One*, *15*(4). https://doi.org/10.1371/journal.pone.0231006

Fan, D., & Kassiri, Z. (2021). Modulation of Cardiac Fibrosis in and Beyond Cells. *Frontiers in Molecular Biosciences*, *8*. https://doi.org/ARTN 750626

10.3389/fmolb.2021.750626

Fan, D., Takawale, A., Basu, R., Patel, V., Lee, J., Kandalam, V., Wang, X., Oudit, G. Y., & Kassiri, Z. (2014). Differential role of TIMP2 and TIMP3 in cardiac hypertrophy, fibrosis, and diastolic dysfunction. *Cardiovascular Research*, *103*(2), 268-280. https://doi.org/10.1093/cvr/cvu072

Fan, D., Takawale, A., Lee, J., & Kassiri, Z. (2012). Cardiac fibroblasts, fibrosis and extracellular matrix remodeling in heart disease. *Fibrogenesis & Tissue Repair*, *5*(1), 15. https://doi.org/10.1186/1755-1536-5-15

Farrell, R. E. (2010). Chapter 17 - cDNA Synthesis. In R. E. Farrell (Ed.), *RNA Methodologies (Fourth Edition)* (pp. 367-384). Academic Press. https://doi.org/https://doi.org/10.1016/B978-0-12-374727-3.00017-6

Forseth, M., Moe, R. O., Kittelsen, K., Skjerve, E., & Toftaker, I. (2023). Comparison of carcass condemnation causes in two broiler hybrids differing in growth rates. *Scientific Reports*, *13*(1). https://doi.org/10.1038/s41598-023-31422-0

Frangogiannis, N. G. (2021). Cardiac fibrosis. *Cardiovascular Research*, *117*(6), 1450-1488. https://doi.org/10.1093/cvr/cvaa324

Frank, D., Kuhn, C., Katus, H. A., & Frey, N. (2006). The sarcomeric Z-disc: a nodal point in signalling and disease. *Journal of Molecular Medicine*, *84*(6), 446-468. https://doi.org/10.1007/s00109-005-0033-1

Frankel, K. A., & Rosser, R. J. (1976). The pathology of the heart in progressive muscular dystrophy: epimyocardial fibrosis. *Human pathology*, *7*(4), 375-386.

Geronimo, B. C., Mastelini, S. M., Carvalho, R. H., Barbon Júnior, S., Barbin, D. F., Shimokomaki, M., & Ida, E. I. (2019). Computer vision system and near-infrared spectroscopy for identification and classification of chicken with wooden breast, and physicochemical and technological characterization. *Infrared Physics & Technology*, *96*, 303-310. https://doi.org/https://doi.org/10.1016/j.infrared.2018.11.036

Gustafsson, Å. B., & Gottlieb, R. A. (2007). Heart mitochondria: gates of life and death. *Cardiovascular Research*, *77*(2), 334-343. https://doi.org/10.1093/cvr/cvm005

Gürtl, B., Kratky, D., Guelly, C., Zhang, L., Gorkiewicz, G., Das, S. K., Tamilarasan, K. P., & Hoefler, G. (2009). Apoptosis and fibrosis are early features of heart failure in an animal model of metabolic cardiomyopathy. *International Journal of Experimental Pathology*, *90*(3), 338-346. https://doi.org/https://doi.org/10.1111/j.1365-2613.2009.00647.x

Havenstein, G. B., Ferket, P. R., & Qureshi, M. A. (2003). Growth, livability, and feed conversion of 1957 versus 2001 broilers when fed representative 1957 and 2001 broiler diets. *Poultry Science*, *82*(10), 1500-1508. https://doi.org/10.1093/ps/82.10.1500

Hein, S., Kostin, S., Heling, A., Maeno, Y., & Schaper, J. (2000). The role of the cytoskeleton in heart failure. *Cardiovascular Research*, *45*(2), 273-278. https://doi.org/10.1016/S0008-6363(99)00268-0

Heling, A., Zimmermann, R., Kostin, S., Maeno, Y., Hein, S., Devaux, B., Bauer, E., Klövekorn, W.-P., Schlepper, M., Schaper, W., & Schaper, J. (2000). Increased Expression of Cytoskeletal, Linkage, and Extracellular Proteins in Failing Human Myocardium. *Circulation research*, *86*(8), 846-853. https://doi.org/doi:10.1161/01.RES.86.8.846

Herum, K. M., Lunde, I. G., Skrbic, B., Florholmen, G., Behmen, D., Sjaastad, I., Carlson, C. R., Gomez, M. F., & Christensen, G. (2013). Syndecan-4 signaling via NFAT regulates extracellular matrix production and cardiac myofibroblast differentiation in response to mechanical stress. *Journal of Molecular and Cellular Cardiology*, *54*, 73-81. https://doi.org/https://doi.org/10.1016/j.yjmcc.2012.11.006

Herum, K. M., Lunde, I. G., Skrbic, B., Louch, W. E., Hasic, A., Boye, S., Unger, A., Brorson, S.-H., Sjaastad, I., & Tønnessen, T. (2015). Syndecan-4 is a key determinant of collagen cross-linking and passive myocardial stiffness in the pressure-overloaded heart. *Cardiovascular Research*, *106*(2), 217-226.

Herum, K. M., Romaine, A., Wang, A., Melleby, A. O., Strand, M. E., Pacheco, J., Braathen, B., Dunér, P., Tønnessen, T., Lunde, I. G., Sjaastad, I., Brakebusch, C., McCulloch, A. D., Gomez, M. F., Carlson, C. R., & Christensen, G. (2020). Syndecan-4 Protects the Heart From the Profibrotic Effects of Thrombin-Cleaved Osteopontin. *J Am Heart Assoc*, *9*(3), e013518. https://doi.org/10.1161/jaha.119.013518

Hilfiker-Kleiner, D., Landmesser, U., & Drexler, H. (2006). Molecular Mechanisms in Heart Failure. *Journal of the American College of Cardiology*, *48*(9_Supplement), A56-A66. https://doi.org/10.1016/j.jacc.2006.07.007

Hinderer, S., & Schenke-Layland, K. (2019). Cardiac fibrosis - A short review of causes and therapeutic strategies. *Advanced Drug Delivery Reviews*, *146*, 77-82. https://doi.org/10.1016/j.addr.2019.05.011

Hung, J.-H., Yang, T.-H., Hu, Z., Weng, Z., & DeLisi, C. (2011). Gene set enrichment analysis: performance evaluation and usage guidelines. *Briefings in Bioinformatics*, *13*(3), 281-291. https://doi.org/10.1093/bib/bbr049

Invitrogen. (2001). *SimplyBlue SafeStain - Fast, Sensitive, and Safe Protein Staining*. Invitrogen life technologies. https://www.thermofisher.com/document-connect/document-connect.html?url=https://assets.thermofisher.com/TFS-Assets%2FLSG%2Fbrochures%2F713_01979_SmplyBlu_bro.pdf

Judge, D. P., Kass, D. A., Thompson, W. R., & Wagner, K. R. (2011). Pathophysiology and Therapy of Cardiac Dysfunction in Duchenne Muscular Dystrophy. *American Journal of Cardiovascular Drugs*, *11*(5), 287-294. https://doi.org/10.2165/11594070-000000000-00000

Kandalam, V., Basu, R., Moore, L., Fan, D., Wang, X. H., Jaworski, D. M., Oudit, G. Y., & Kassiri, Z. (2011). Lack of Tissue Inhibitor of Metalloproteinases 2 Leads to Exacerbated Left Ventricular Dysfunction and Adverse Extracellular Matrix Remodeling in Response to Biomechanical Stress. *Circulation*, *124*(19), 2094-U2152. https://doi.org/10.1161/Circulationaha.111.030338

Kemp, C. D., & Conte, J. V. (2012). The pathophysiology of heart failure. *Cardiovascular Pathology*, *21*(5), 365-371. https://doi.org/https://doi.org/10.1016/j.carpath.2011.11.007

Kong, P., Christia, P., & Frangogiannis, N. G. (2014). The pathogenesis of cardiac fibrosis. *Cellular and Molecular Life Sciences*, *71*(4), 549-574. https://doi.org/10.1007/s00018-013-1349-6

Kostin, S., Hein, S., Arnon, E., Scholz, D., & Schaper, J. (2000). The Cytoskeleton and Related Proteins in the Human Failing Heart. *Heart Failure Reviews*, *5*(3), 271-280. https://doi.org/10.1023/A:1009813621103

Kothari, V., & Mathews, S. T. (2015). Detection of Blotted Proteins: Not All Blockers Are Created Equal. In B. T. Kurien & R. H. Scofield (Eds.), *Detection of Blotted Proteins: Methods and Protocols* (pp. 27-32). Springer New York. https://doi.org/10.1007/978-1-4939-2718-0_4

Kurien, B. T., & Scofield, R. H. (2015). Western blotting: an introduction. *Methods Mol Biol*, *1312*, 17-30. https://doi.org/10.1007/978-1-4939-2694-7_5

Lechner, A., Herzig, J. J., Kientsch, J. G., Kohler, M., Bloch, K. E., Ulrich, S., & Schwarz, E. I. (2023). Cardiomyopathy as cause of death in Duchenne muscular dystrophy: a longitudinal observational study. *Erj Open Research*, *9*(5). https://doi.org/Artn 176

10.1183/23120541.00176-2023

Li, A., Gao, M., Jiang, W., Qin, Y., & Gong, G. (2020). Mitochondrial Dynamics in Adult Cardiomyocytes and Heart Diseases [Review]. *Frontiers in Cell and Developmental Biology*, *8*. https://doi.org/10.3389/fcell.2020.584800

Li, L., Zhao, Q., & Kong, W. (2018). Extracellular matrix remodeling and cardiac fibrosis. *Matrix Biology*, *68-69*, 490-506. https://doi.org/10.1016/j.matbio.2018.01.013

Li, X., Zhang, W., Cao, Q., Wang, Z., Zhao, M., Xu, L., & Zhuang, Q. (2020). Mitochondrial dysfunction in fibrotic diseases. *Cell Death Discovery*, *6*(1), 80. https://doi.org/10.1038/s41420-020-00316-9

Liu, M., Lv, J., Pan, Z., Wang, D., Zhao, L., & Guo, X. (2022). Mitochondrial dysfunction in heart failure and its therapeutic implications [Review]. *Frontiers in Cardiovascular Medicine*, *9*. https://doi.org/10.3389/fcvm.2022.945142

Lockhart, M., Wirrig, E., Phelps, A., & Wessels, A. (2011). Extracellular matrix and heart development. *Birth Defects Research Part A: Clinical and Molecular Teratology*, *91*(6), 535-550. https://doi.org/https://doi.org/10.1002/bdra.20810

López, B., González, A., Hermida, N., Valencia, F., Teresa, E. d., & Díez, J. (2010). Role of lysyl oxidase in myocardial fibrosis: from basic science to clinical aspects. *American Journal of Physiology-Heart and Circulatory Physiology*, *299*(1), H1-H9. https://doi.org/10.1152/ajpheart.00335.2010

Lunde, I. G., Herum, K. M., Carlson, C. C., & Christensen, G. (2016). Syndecans in heart fibrosis. *Cell and Tissue Research*, *365*(3), 539-552. https://doi.org/10.1007/s00441-016-2454-2

Macfelda, K., Kapeller, B., Wilbacher, I., & Losert, U. M. (2007). Behavior of Cardiomyocytes and Skeletal Muscle Cells on Different Extracellular Matrix Components—Relevance for Cardiac Tissue Engineering. *Artificial Organs*, *31*(1), 4-12. https://doi.org/https://doi.org/10.1111/j.1525-1594.2007.00334.x

Martinez, M. G., Bullock, A. J., MacNeil, S., & Rehman, I. U. (2019). Characterisation of structural changes in collagen with Raman spectroscopy. *Applied Spectroscopy Reviews*, *54*(6), 509-542. https://doi.org/10.1080/05704928.2018.1506799

Mazur, W., Hor, K. N., Germann, J. T., Fleck, R. J., Al-Khalidi, H. R., Wansapura, J. P., Chung, E. S., Taylor, M. D., Jefferies, J. L., & Woodrow Benson, D. (2012). Patterns of left ventricular remodeling in patients with Duchenne muscular dystrophy: a cardiac MRI study of ventricular geometry, global function, and strain. *The international journal of cardiovascular imaging*, *28*, 99-107.

Mazzoni, M., Petracci, M., Meluzzi, A., Cavani, C., Clavenzani, P., & Sirri, F. (2015). Relationship between pectoralis major muscle histology and quality traits of chicken meat. *Poultry Science*, *94*(1), 123-130. https://doi.org/https://doi.org/10.3382/ps/peu043

Mesnard-Rouiller, L., Mercadier, J.-J., Butler-Browne, G., Heimburger, M., Logeart, D., Allen, P. D., & Samson, F. (1997). Troponin T mRNA and Protein Isoforms in the Human Left Ventricle: Pattern of Expression in Failing and Control Hearts. *Journal of Molecular and Cellular Cardiology*, *29*(11), 3043-3055. https://doi.org/https://doi.org/10.1006/jmcc.1997.0519

Mohammadzadeh, N., Lunde, I. G., Andenæs, K., Strand, M. E., Aronsen, J. M., Skrbic, B., Marstein, H. S., Bandlien, C., Nygård, S., & Gorham, J. (2019). The extracellular matrix proteoglycan lumican improves survival and counteracts cardiac dilatation and failure in mice subjected to pressure overload. *Scientific Reports*, *9*(1), 9206.

Monici, M. (2005). Cell and tissue autofluorescence research and diagnostic applications. In *Biotechnology Annual Review* (Vol. 11, pp. 227-256). Elsevier. https://doi.org/https://doi.org/10.1016/S1387-2656(05)11007-2

Moriuchi, T., Kagawa, N., Mukoyama, M., & Hizawa, K. (1993). Autopsy analyses of the muscular dystrophies. *The Tokushima journal of experimental medicine*, *40*(1-2), 83-93.

Ngu, J. M. C., Teng, G., Meijndert, H. C., Mewhort, H. E., Turnbull, J. D., Stetler-Stevenson, W. G., & Fedak, P. W. M. (2014). Human cardiac fibroblast extracellular matrix remodeling: dual effects of tissue inhibitor of metalloproteinase-2. *Cardiovascular Pathology*, *23*(6), 335-343. https://doi.org/https://doi.org/10.1016/j.carpath.2014.06.003

Nowakowski, A. B., Wobig, W. J., & Petering, D. H. (2014). Native SDS-PAGE: high resolution electrophoretic separation of proteins with retention of native properties

including bound metal ions. *Metallomics*, *6*(5), 1068-1078. https://doi.org/10.1039/c4mt00033a

Olkowski, A. A., Wojnarowicz, C., Rathgeber, B. M., Abbott, J. A., & Classen, H. L. (2003). Lesions of the pericardium and their significance in the aetiology of heart failure in broiler chickens. *Research in Veterinary Science*, *74*(3), 203-211. https://doi.org/https://doi.org/10.1016/S0034-5288(03)00004-3

Orlando, A., Franceschini, F., Muscas, C., Pidkova, S., Bartoli, M., Rovere, M., & Tagliaferro, A. (2021). A Comprehensive Review on Raman Spectroscopy Applications. *Chemosensors*, *9*(9), 262. https://www.mdpi.com/2227-9040/9/9/262

Pejšková, L., Rønning, S. B., Kent, M. P., Solberg, N. T., Høst, V., Thu-Hien, T., Wold, J. P., Lunde, M., Mosleth, E., Pisconti, A., Kolset, S. O., Carlson, C. R., & Pedersen, M. E. (2023). Characterization of wooden breast myopathy: a focus on syndecans and ECM remodeling. *Front Physiol*, *14*, 1301804. https://doi.org/10.3389/fphys.2023.1301804

Petracci, M., Mudalal, S., Soglia, F., & Cavani, C. (2015). Meat quality in fast-growing broiler chickens. *World's Poultry Science Journal*, *71*(2), 363-374. https://doi.org/10.1017/S0043933915000367

Petracci, M., Soglia, F., Madruga, M., Carvalho, L., Ida, E., & Estévez, M. (2019). Wooden-Breast, White Striping, and Spaghetti Meat: Causes, Consequences and Consumer Perception of Emerging Broiler Meat Abnormalities. *Comprehensive Reviews in Food Science and Food Safety*, *18*(2), 565-583. https://doi.org/10.1111/1541-4337.12431

Pillai-Kastoori, L., Schutz-Geschwender, A. R., & Harford, J. A. (2020). A systematic approach to quantitative Western blot analysis. *Analytical Biochemistry*, *593*, 113608. https://doi.org/https://doi.org/10.1016/j.ab.2020.113608

Ponikowski, P., Anker, S. D., AlHabib, K. F., Cowie, M. R., Force, T. L., Hu, S., Jaarsma, T., Krum, H., Rastogi, V., Rohde, L. E., Samal, U. C., Shimokawa, H., Budi Siswanto, B., Sliwa, K., & Filippatos, G. (2014). Heart failure: preventing disease and death worldwide. *ESC Heart Failure*, *1*(1), 4-25. https://doi.org/https://doi.org/10.1002/ehf2.12005

Prieto, N., Pawluczyk, O., Dugan, M. E. R., & Aalhus, J. L. (2017). A Review of the Principles and Applications of Near-Infrared Spectroscopy to Characterize Meat, Fat, and Meat Products. *Applied Spectroscopy*, *71*(7), 1403-1426. https://doi.org/10.1177/0003702817709299

Purslow, P. P. (2008). The Extracellular Matrix of Skeletal and Cardiac Muscle. In P. Fratzl (Ed.), *Collagen: Structure and Mechanics* (pp. 325-357). Springer US. https://doi.org/10.1007/978-0-387-73906-9_12

Rooprai, H., Rucklidge, G., Panou, C., & Pilkington, G. (2000). The effects of exogenous growth factors on matrix metalloproteinase secretion by human brain tumour cells. *British journal of cancer*, *82*(1), 52-55.

Rosca, M. G., & Hoppel, C. L. (2013). Mitochondrial dysfunction in heart failure. *Heart Failure Reviews*, *18*(5), 607-622. https://doi.org/10.1007/s10741-012-9340-0

Sander, H., Wallace, S., Plouse, R., Tiwari, S., & Gomes, A. V. (2019). Ponceau S waste: Ponceau S staining for total protein normalization. *Analytical Biochemistry*, *575*, 44-53. https://doi.org/10.1016/j.ab.2019.03.010

Sarantitis, I., Papanastasopoulos, P., Manousi, M., Baikoussis, N. G., & Apostolakis, E. (2012). The Cytoskeleton of the Cardiac Muscle Cell. *Hellenic Journal of Cardiology*, *53*(5), 367-379. <Go to ISI>://WOS:000310476200006

Schaefer, L., Babelova, A., Kiss, E., Hausser, H.-J., Baliova, M., Krzyzankova, M., Marsche, G., Young, M. F., Mihalik, D., & Götte, M. (2005). The matrix component biglycan is proinflammatory and signals through Toll-like receptors 4 and 2 in macrophages. *The Journal of clinical investigation*, *115*(8), 2223-2233.

Schmid, J., Liesinger, L., Birner-Gruenberger, R., Stojakovic, T., Scharnagl, H., Dieplinger, B., Asslaber, M., Radl, R., Beer, M., Polacin, M., Mair, J., Szolar, D., Berghold, A., Quasthoff, S., Binder, J. S., & Rainer, P. P. (2018). Elevated Cardiac Troponin T in Patients With Skeletal Myopathies. *Journal of the American College of Cardiology*, *71*(14), 1540-1549. https://doi.org/10.1016/j.jacc.2018.01.070

Schmittgen, T. D., & Livak, K. J. (2008). Analyzing real-time PCR data by the comparative C(T) method. *Nat Protoc*, *3*(6), 1101-1108. https://doi.org/10.1038/nprot.2008.73

Scientific, T. (2014). *Real-time PCR handbook*. Thermo Fisher Scientific. https://www.thermofisher.com/content/dam/LifeTech/global/Forms/PDF/real-time-pcr-handbook.pdf

Sequeira, V., Nijenkamp, L. L. A. M., Regan, J. A., & van der Velden, J. (2014). The physiological role of cardiac cytoskeleton and its alterations in heart failure. *Biochimica et Biophysica Acta (BBA) - Biomembranes*, *1838*(2), 700-722. https://doi.org/https://doi.org/10.1016/j.bbamem.2013.07.011

Severs, N. J. (2000). The cardiac muscle cell. *BioEssays*, *22*(2), 188-199. https://doi.org/https://doi.org/10.1002/(SICI)1521-1878(200002)22:2<188::AID-BIES10>3.0.CO;2-T

Shah, S., Gnanasegaran, G., Sundberg-Cohon, J., & Buscombe, J. R. (2009). The Heart: Anatomy, Physiology and Exercise Physiology. In A. Movahed, G. Gnanasegaran, J. Buscombe, & M. Hall (Eds.), *Integrating Cardiology for Nuclear Medicine Physicians: A Guide to Nuclear Medicine Physicians* (pp. 3-22). Springer Berlin Heidelberg. https://doi.org/10.1007/978-3-540-78674-0_1

Siasos, G., Tsigkou, V., Kosmopoulos, M., Theodosiadis, D., Simantiris, S., Tagkou, N. M., Tsimpiktsioglou, A., Stampouloglou, P. K., Oikonomou, E., Mourouzis, K., Philippou, A., Vavuranakis, M., Stefanadis, C., Tousoulis, D., & Papavassiliou, A. G. (2018). Mitochondria and cardiovascular diseases-from pathophysiology to treatment. *Ann Transl Med*, *6*(12), 256. https://doi.org/10.21037/atm.2018.06.21

Sihvo, H. K., Immonen, K., & Puolanne, E. (2014). Myodegeneration With Fibrosis and Regeneration in the Pectoralis Major Muscle of Broilers. *Veterinary Pathology*, *51*(3), 619-623. https://doi.org/10.1177/0300985813497488

Soglia, F., Mudalal, S., Babini, E., Di Nunzio, M., Mazzoni, M., Sirri, F., Cavani, C., & Petracci, M. (2016). Histology, composition, and quality traits of chicken Pectoralis major muscle affected by wooden breast abnormality. *Poultry Science*, *95*(3), 651-659. https://doi.org/https://doi.org/10.3382/ps/pev353

Soneson, C., & Delorenzi, M. (2013). A comparison of methods for differential expression analysis of RNA-seq data. *Bmc Bioinformatics*, *14*. https://doi.org/Artn 91

10.1186/1471-2105-14-91

Strand, M. E., Herum, K. M., Rana, Z. A., Skrbic, B., Askevold, E. T., Dahl, C. P., Vistnes, M., Hasic, A., Kvaløy, H., Sjaastad, I., Carlson, C. R., Tønnessen, T., Gullestad, L., Christensen, G., & Lunde, I. G. (2013). Innate immune signaling induces expression and shedding of the heparan sulfate proteoglycan syndecan-4 in cardiac fibroblasts and myocytes, affecting inflammation in the pressure-overloaded heart. *The FEBS Journal*, *280*(10), 2228-2247. https://doi.org/https://doi.org/10.1111/febs.12161

Støle, T. P., Lunde, M., Shen, X., Martinsen, M., Lunde, P. K., Li, J., Lockwood, F., Sjaastad, I., Louch, W. E., Aronsen, J. M., Christensen, G., & Carlson, C. R. (2022). The female syndecan-4−/− heart has smaller cardiomyocytes, augmented insulin/pSer473-Akt/pSer9-GSK-3β signaling, and lowered SCOP, pThr308-Akt/Akt and GLUT4 levels [Original Research]. *Frontiers in Cell and Developmental Biology*, *10*. https://doi.org/10.3389/fcell.2022.908126

Takawale, A., Zhang, P., Patel, V. B., Wang, X. H., Oudit, G., & Kassiri, Z. (2017). Tissue Inhibitor of Matrix Metalloproteinase-1 Promotes Myocardial Fibrosis by Mediating CD63-Integrin β1 Interaction. *Hypertension*, *69*(6), 1092-+. https://doi.org/10.1161/Hypertensionaha.117.09045

Tanai, E., & Frantz, S. (2016). Pathophysiology of Heart Failure. *Comprehensive Physiology*, *6*(1), 187-214. https://doi.org/10.1002/cphy.c140055

Tansey, D. K., Aly, Z., & Sheppard, M. N. (2005). Fat in the right ventricle of the normal heart. *Histopathology*, *46*(1), 98-104. https://doi.org/10.1111/j.1365-2559.2005.02054.x

Torrealba, N., Aranguiz, P., Alonso, C., Rothermel, B. A., & Lavandero, S. (2017). Mitochondria in Structural and Functional Cardiac Remodeling. In G. Santulli (Ed.),

Mitochondrial Dynamics in Cardiovascular Medicine (pp. 277-306). Springer International Publishing. https://doi.org/10.1007/978-3-319-55330-6_15

Tsai, C.-L., Chen, J.-C., & Wang, W.-J. (2001). Near-infrared absorption property of biological soft tissue constituents. *Journal of Medical and Biological Engineering*, *21*(1), 7-14.

Tyagi, S. C., Kumar G, S., & Glover, G. (1995). Induction of tissue inhibitor and matrix metalloproteinase by serum in human heart-derived fibroblast and endomyocardial endothelial cells. *Journal of cellular biochemistry*, *58*(3), 360-371.

van Westering, T. L., Betts, C. A., & Wood, M. J. (2015). Current understanding of molecular pathology and treatment of cardiomyopathy in duchenne muscular dystrophy. *Molecules*, *20*(5), 8823-8855. https://doi.org/10.3390/molecules20058823

Velleman, S. G. (2015). Relationship of skeletal muscle development and growth to breast muscle myopathies: a review. *Avian Diseases*, *59*(4), 525-531.

Velleman, S. G., & Clark, D. L. (2015). Histopathologic and Myogenic Gene Expression Changes Associated with Wooden Breast in Broiler Breast Muscles. *Avian Diseases*, *59*(3), 410-418. https://www.jstor.org/stable/26431070

Velleman, S. G., & Song, Y. (2017). Development and growth of the avian pectoralis major (breast) muscle: function of syndecan-4 and glypican-1 in adult myoblast proliferation and differentiation. *Frontiers in physiology*, *8*, 273408.

Verdejo, H. E., del Campo, A., Troncoso, R., Gutierrez, T., Toro, B., Quiroga, C., Pedrozo, Z., Munoz, J. P., Garcia, L., Castro, P. F., & Lavandero, S. (2012). Mitochondria, Myocardial Remodeling, and Cardiovascular Disease. *Current Hypertension Reports*, *14*(6), 532-539. https://doi.org/10.1007/s11906-012-0305-4

Walcher, T., Steinbach, P., Spieß, J., Kunze, M., Gradinger, R., Walcher, D., & Bernhardt, P. (2011). Detection of long-term progression of myocardial fibrosis in Duchenne muscular dystrophy in an affected family: A cardiovascular magnetic resonance study. *European Journal of Radiology*, *80*(1), 115-119. https://doi.org/https://doi.org/10.1016/j.ejrad.2010.07.005

Wang, X., Berry, E., Hernandez-Anzaldo, S., Takawale, A., Kassiri, Z., & Fernandez-Patron, C. (2015). Matrix Metalloproteinase-2 Mediates a Mechanism of Metabolic Cardioprotection Consisting of Negative Regulation of the Sterol Regulatory Element–Binding Protein-2/3-Hydroxy-3-Methylglutaryl-CoA Reductase Pathway in the Heart. *Hypertension*, *65*(4), 882-888. https://doi.org/doi:10.1161/HYPERTENSIONAHA.114.04989

Wittig, J. G., & Münsterberg, A. (2020). The Chicken as a Model Organism to Study Heart Development. *Cold Spring Harbor Perspectives in Biology*, *12*(8). https://doi.org/ARTN a037218

10.1101/cshperspect.a037218

Wold, J. P., Måge, I., Løvland, A., Sanden, K. W., & Ofstad, R. (2019). Near-infrared spectroscopy detects woody breast syndrome in chicken fillets by the markers protein content and degree of water binding. *Poultry Science*, *98*(1), 480-490. https://doi.org/https://doi.org/10.3382/ps/pey351

Xie, X., Wu, S. P., Tsai, M. J., & Tsai, S. (2017). The Role of COUP-TFII in Striated Muscle Development and Disease. *Curr Top Dev Biol*, *125*, 375-403. https://doi.org/10.1016/bs.ctdb.2016.12.006

Xing, T., Luo, D., Zhao, X., Xu, X., Li, J., Zhang, L., & Gao, F. (2021). Enhanced cytokine expression and upregulation of inflammatory signaling pathways in broiler chickens affected by wooden breast myopathy. *Journal of the Science of Food and Agriculture*, *101*(1), 279-286. https://doi.org/https://doi.org/10.1002/jsfa.10641

Xing, T., Zhao, X., Zhang, L., Li, J., Zhou, G., Xu, X., & Gao, F. (2020). Characteristics and incidence of broiler chicken wooden breast meat under commercial conditions in China. *Poultry Science*, *99*(1), 620-628.

Xing, T., Zhao, Z. R., Zhao, X., Xu, X. L., Zhang, L., & Gao, F. (2021). Enhanced transforming growth factor-beta signaling and fibrosis in the pectoralis major muscle of broiler chickens affected by wooden breast myopathy. *Poultry Science*, *100*(3), 100804. https://doi.org/https://doi.org/10.1016/j.psj.2020.10.058

Zanotti, S., Negri, T., Cappelletti, C., Bernasconi, P., Canioni, E., Di Blasi, C., Pegoraro, E., Angelini, C., Ciscato, P., & Prelle, A. (2005). Decorin and biglycan expression is differentially altered in several muscular dystrophies. *Brain*, *128*(11), 2546-2555.

Zhang, Y., Wang, P., Xu, X., Xia, T., Li, Z., & Zhao, T. (2020). Effect of wooden breast myopathy on water-holding capacity and rheological and gelling properties of chicken broiler breast batters. *Poultry Science*, *99*(7), 3742-3751. https://doi.org/https://doi.org/10.1016/j.psj.2020.03.032

Zhou, Z., Arroum, T., Luo, X., Kang, R., Lee, Y. J., Tang, D., Hüttemann, M., & Song, X. (2024). Diverse functions of cytochrome c in cell death and disease. *Cell Death & Differentiation*. https://doi.org/10.1038/s41418-024-01284-8

Zhu, F. Y., Li, P., & Sheng, Y. H. (2022). Treatment of myocardial interstitial fibrosis in pathological myocardial hypertrophy. *Frontiers in Pharmacology*, *13*. https://doi.org/ARTN 1004181

10.3389/fphar.2022.1004181

Zuidhof, M. J., Schneider, B. L., Carney, V. L., Korver, D. R., & Robinson, F. E. (2014). Growth, efficiency, and yield of commercial broilers from 1957, 1978, and 2005. *Poult Sci*, *93*(12), 2970-2982. https://doi.org/10.3382/ps.2014-04291

9. Attachments

Table A. Laboratory equipment used in the different analyses.

Equipment	Supplier
Adhesive Sealing Sheets	Thermo Fisher Scientific
Biosphere®Filter Tips 0.1-10µL	Sarstedt
Bolt™Bis-Tris Mini Protein Gel 4-12%	Thermo Fisher Scientific
Combitips advanced®0.5mL	Eppendorf
E1-ClipTip	Thermo Fisher Scientific
Eppendorf tubes	Eppendorf
Falcon tubes(50mL)	VWR
Gelloader Pipette Tips 1-200µL	Sarstedt
iBlot™3 Transfer Stacks Midi NC	Thermo Fisher Scientific
NuPAGE™ 10% and 12% Bis-Tris gels	Thermo Fisher Scientific
MicroAmp™Optical Adhesive Film	Thermo Fisher Scientific
Multipiette®E3	Eppendorf
Quality Pipette Tips 20-300 µL	Sarstedt
Sterile ClipTip	Thermo Fischer Scientific

Table B. The instruments used in the various analyses.

Instrument	Supplier
Epson Perfection 4990 Photo	Epson
G:BOX Chemi XX6/XX9	Syngene
GeneAmp® PCR System 9700	Thermo Fisher Scientific
Heraus MegaFuge 8	Thermo Fisher Scientific
HS501 digital	IKA

iBlot 3	Thermo Fischer Scientific
MicroAmp®Optical 96-, 384-well Reaction Plate	Life technologies™
MicroStar 17R	VWR
NanoDrop One	Thermo Fisher Scientific
QuantiStudio 5	Thermo Fisher Scientific
Rollermixer SRT9D	Stuart
PowerEase500	Invitrogen
Precellys Evolution	Bertin Technologies
Seesaw Rocker SSL4	Stuart
ThermoMixer F1.5	Eppendorf

Table C. Solutions used to execute the experiments.

Solutions	**Supplier**
BenchMark™Prestain Protein Ladder	Thermo Fisher Scientific
Bolt™LDS Sample Buffer(4X)	Life technologies™
Bolt™MOPS SDS Running Buffer(20X)	Thermo Fisher Scientific
ECL™Plex Fluorescent Rainbow Marker	Cytiva
ECL Prime™blocking agent	Cytiva
Luna®Universal Probe qPCR Mix	New England Biolabs®
MEA-SDS running buffer (20X)	Thermo Fisher Scientific
NuPAGE™MOPS SDS Running Buffer (20X)	Thermo Fisher Scientific
Ponceau S solution	Sigma Aldrich
TBS-Tween™tablets	Medicago

Table D. Target specific TaqMan probes used in the qPCR analysis.

TaqMan Probes	Assay ID
Actin Alpha 2	Gg03352404_m1
Biglycan	Gg07177841_m1
Collagen type 1	Gg07167955_g1
Collagen type 3	Gg03325764_m1
Decorin	Gg03355063_m1
Desmin	Gg03330588_m1
Eucaryotic translation elongation factor2	Gg03339740_m1
Interleukine 1 beta	Gg03347157_g1
Lysyl Oxidase	Gg03340182_m1
Lumican	Gg03325844_m1
Matrix metalloproteinase-2	Gg03365277_m1
Matrix metalloproteinase-9	Gg03338324_g1
Platelet-derived growth factor R Beta	Gg07165531_s1
Syndecan-1	Gg07175697_s1
Syndecan-2	Gg03345645_m1

Syndecan-3	Gg03339851_m1
Syndecan-4	Gg03370419_m1
Transforming growth factor beta 1	Gg07156069_g1
Tissue inhibitor of metalloproteinases 2	Gg07157666_m1
Toll-like receptor 4	Gg03354643_m1
Tropomyosin beta-chain	Gg03815778_s1
Troponin T2 cardiac type	Gg03371505_m1
Tubulin alfa-1	Gg07162375_m1
Tubulin beta-1	Gg03371486_g1

Table E. Software that was used to carry out various analyses.

Software	**Supplier**
Adobe Illustrator	Adobe Systems
Biorender	Science Suite Inc
GraphPad Prism 10.2.2	GraphPad Software
ImageQuant™TL	GE Healthcare
Microsoft Excel Office (2021)	Microsoft
R-Studio	Posit, PBC
Unscrambler X	CAMO Software

Table F. Antibodies used for western blotting.

Antibodies	**Product number**	**Supplier**
Actin	ab1801	Abcam
α -tubulin	T5168	Sigma-Aldrich
β I Tubulin (EPR16778) TUBB1	ab179511	Abcam
ECL™Plex goat-a-mouse IgG, Cy™3	PA43009	Cytiva
ECL™Plex goat-a-rabbit IgG, Cy™5	PA45011	Cytiva
GAPDH	sc-47724	Santa Cruz
MMP2	AB181286	Abcam
MMP9	NBP1-57940	Novusbiologica
TIMP-1 (G-6)	sc-365905	Santa Cruz
TIMP2	NP003246.1	MyBiosource
Troponin T (JLT-12)	T6277	Sigma-Aldrich
Troponin T Cardiac	MA5-12960	Invitrogen/ThermoFisher
Vinculin	V9131	Sigma-Aldrich

Table G. Kits used in the different analyses.

Kit	**Supplier**
iBlot™Gel Transfer Stacks Midi NC	Thermo Fisher Scientific
iBlot™Gel Transfer Stacks Nitrocellulose, Regular	Thermo Fisher Scientific

LunaScript®RT SuperMix Kit	New England Biolabs®
Micro BCA protein assay kit	Thermo Fisher Scientific
RNAeasy®Mini Kit (50)	Qiagen